JOURNAL OF AGRICULTURAL AND FOOD CHEMISTRY

Article

Cite This: J. Agric. Food Chem. XXXX, XXX, XXX−XXX

pubs.acs.org/JAFC

Encapsulation and Stabilization of α-Lipoic Acid in Cyclodextrin Inclusion Complex Electrospun Nanofibers: Antioxidant and Fast-Dissolving α-Lipoic Acid/Cyclodextrin Nanofibrous Webs

Asli Celebioglu* and Tamer Uyar*

Department of Fiber Science & Apparel Design, College of Human Ecology, Cornell University, Ithaca, New York 14853, United States

Supporting Information

ABSTRACT: In this study, electrospinning of nanofibers from alpha-lipoic acid/cyclodextrin inclusion complex systems was successfully performed without having any polymeric matrix. Alpha-lipoic acid (α-LA) is a natural antioxidant compound which is widely used as a food supplement. However, it has limited water solubility and poor thermal and oxidative stability. Nevertheless, it is possible to enhance its water solubility and thermal stability by inclusion complexation with cyclodextrins. Here, hydroxypropyl-beta-cyclodextrin (HP-β-CyD) and hydroxypropyl-gamma-cyclodextrin (HP-γ-CyD) were chosen as host molecules for forming inclusion complexation with α-LA. Accordingly, α-LA was inclusion complexed with HP-β-CyD and HP-γ-CyD by using very high concentrated aqueous solutions of CyD (200%, w/v) having 1/1 and 2/1 molar ratio of α-LA/CyD. Except α-LA/HP-β-CyD (1/1) solution, other α-LA/CyD solutions were turbid indicating the presence of some noncomplexed α-LA whereas α-LA/HP-β-CyD (1/1) solution was very homogeneous signifying that α-LA was fully complexed with HP-β-CyD. Even so, electrospinning was performed for all of the α-LA/HP-β-CyD (1/1 and 2/1) and α-LA/HP-γ-CyD (1/1 and 2/1) aqueous solutions, and defect-free bead-less and uniform nanofibers were successfully obtained for all of the α-LA/CyD solutions. However, the electrospinning process for α-LA/CyD (1/1) systems was much more efficient than the α-LA/CyD (2/1) systems, and we were able to produce self-standing and flexible nanofibrous webs from α-LA/CyD (1/1) systems. α-LA was efficiently preserved during the electrospinning process of α-LA/CyD (1/1) systems and the resulting electrospun α-LA/HP-β-CyD and α-LA/HP-γ-CyD nanofibers were produced with the molar ratios of ∼1/1 and ∼0.85/1 (α-LA/CyD), respectively. The better encapsulation efficiency of α-LA in α-LA/HP-β-CyD nanofibers was due to higher solubility increase and higher binding strength between α-LA and HP-β-CyD as revealed by the phase solubility test. α-LA was in the amorphous state in α-LA/CyD nanofibers and both α-LA/HP-β-CyD and α-LA/HP-γ-CyD nanofibers were dissolved very quickly in water and also when they wetted with artificial saliva. Additionally, the antioxidant activity of pure α-LA and α-LA/CyD nanofibers was comparatively evaluated using ABTS radical cation assay. α-LA/CyD nanofibers have shown significantly higher antioxidant performance compared to pure α-LA owing to improved water solubility by CyD inclusion complexation. The thermal stability enhancement of α-LA in α-LA/CyD nanofibers was achieved compared to pure α-LA under heat treatment (100 °C for 24 h). These promising results support that antioxidant α-LA/CyD nanofibers may have potential applications as orally fast-dissolving food supplements.

KEYWORDS: *alpha-lipoic acid, hydroxypropyl-beta-cyclodextrin, hydroxypropyl-gamma-cyclodextrin, electrospinning, nanofibers, fast-dissolving, food*

INTRODUCTION

Alpha-lipoic acid (α-LA) is a eight-carbon cyclic disulfide compound, and due to its important role as a cofactor in energy metabolism and high antioxidant activity,[1,2] α-LA is used as a dietary supplement.[3] However, α-LA has poor water solubility and it is not stable under thermal process; therefore, encapsulation of α-LA is of interest in order to improve its thermal and oxidative stability and enhance its solubility and bioavailability.[4,5] Cyclodextrins are cyclic oligosaccharides produced from starch and they are well-known for their molecular encapsulation capability by forming inclusion complexes with bioactive molecules; therefore, they are used in foods.[6−9] The solubility and bioavailability of the bioactive compounds (e.g., essential oils, vitamins, flavors, food supplements, etc.) can be enhanced by cyclodextrin inclusion complexation.[6−9] In addition, cyclodextrins improve thermal and oxidative stability, control the release, mask the bitter taste, prevent the loss during storage, and provide longer shelf life for such bioactive compounds.[6,8] The molecular encapsulation of α-LA by cyclodextrin inclusion complexation has also been reported in order to improve the stability, bioavailability, and aqueous solubility of α-LA.[10−17] There is also a commercially available product of α-LA/cyclodextrin on the market (R-ALA Cyclodextrin Complex Powder; https://nootropicsdepot.com/r-ala-cyclodextrin-complex-powder/).

Recently, electrospinning technique has been widely investigated in the literature as a very promising nano-

Received: September 5, 2019
Revised: October 26, 2019
Accepted: November 6, 2019
Published: November 6, 2019

DOI: 10.1021/acs.jafc.9b05580
J. Agric. Food Chem. XXXX, XXX, XXX−XXX

encapsulation approach for encapsulation of bioactive compounds (e.g., essential oils, vitamins, flavors, food supplements, etc.) for food industries.[18−23] There are a variety of techniques such as spray drying, freeze-drying, coacervation, emulsification, melt extrusion, etc. available for encapsulation of bioactive molecules for the purpose of food preservation, but each of these encapsulation techniques has their own merits and drawbacks.[24] For instance, spray drying is one of the widely used technique for microencapsulation of bioactive food additives, however, spray drying process uses relatively high drying temperatures where the heat sensitive food ingredients may degrade during this process. In case of coacervation and emulsification techniques, mostly microparticles are obtained in the solutions, which further require proper drying technique to produce encapsulated food ingredients in powder forms. Electrospinning is a facile nanoencapsulation technique for food applications, which offers several advantages over other techniques including very convenient incorporation of bioactive molecules into nanofiber matrix with high encapsulation efficiency.[18−23] More importantly, the nanofibers encapsulating bioactive agents are produced at ambient conditions without the need of high temperature during the electrospinning process, which is considered the key advantage especially for encapsulating heat-labile bioactive compounds. The electrospun nanofibers possess several structural advantages, such as nanoscale fiber diameters along with tunable fiber diameter, very high surface-to-volume ratio and nanoporosity. Such structural advantages of electrospun nanofibers provide enhanced stability and bioavailability and the controlled delivery of the encapsulated bioactive compounds.[18−23] Typically, bioactive compounds are either dissolved or dispersed in a common solution with edible polymeric materials and the electrospinning of such bioactive compound/polymer solution system is carried out under high electrical field at ambient conditions (at room temperature, atmospheric pressure, etc.). The electrospinning process mostly produces nanofibers having dimeters less than micron and the bioactive compounds are efficiently encapsulated within nanofiber matrix. Unlike the polymeric films, the electrospun nanofibrous structures are produced in the form of web/mat/membrane having nanoporous structure, very high surface area and very lightweight. The electrospun nanofibrous webs have also self-standing and flexible characteristics. The electrospun nanofibrous webs produced from hydrophilic edible biopolymers encapsulating bioactive compounds would readily dissolve or disintegrate in water. Hence, electrospun nanofibrous web/mat/membrane materials encapsulating bioactive compounds can be quite promising for designing orally fast-dissolving delivery systems for pharmaceutics[25,26] and food industries.[27−38] Very recently, we have shown that nanofibrous webs having fast-dissolving properties can be simply produced from purely cyclodextrin inclusion complexes with some essential oils[27,28,31−37] and flavors[29,38] and vitamins[30] by polymer-free electrospinning. Cyclodextrins, especially modified cyclodextrins (hydroxypropylated-cyclodextrins, methylated-cyclodextrins and sulfobutylated-cyclodextrins, etc.) are highly water-soluble (more than 200 gr/100 mL),[39] therefore, the choice of using cyclodextrins both as a nanofiber matrix for encapsulating bioactive molecules and for the inclusion complexation with these bioactive molecules offers certain advantages. For instance, nanofibers made purely from cyclodextrin inclusion complexes would have fast-dissolving character and, also, the bioactive molecules would have greater water solubility and very high thermal stability and prolonged shelf life due to cyclodextrin inclusion complexation.[27−38]

Variety of bioactive compounds (e.g., essential oils, vitamins, flavors, food supplements, etc.) have been encapsulated within nanofiber matrix by electrospinning for food related applications.[18−23] Yet, to the best of our knowledge, no study has been reported related to encapsulation of α-LA in electrospun nanofiber matrix. More importantly, this study summarizes our effort to develop fast-dissolving α-LA/cyclodextrin inclusion complex nanofibrous webs by polymer-free electrospinning. For this purpose, we have chosen two types of hydroxypropylated-cyclodextrins (hydroxypropyl-beta-cyclodextrin (HP-β-CyD) and hydroxypropyl-gamma-cyclodextrin (HP-γ-CyD)) for the inclusion complexation with α-LA. Both of these hydroxypropylated-cyclodextrins (HP-β-CyD and HP-γ-CyD) are highly water-soluble and the electrospinning of nanofibers from HP-β-CyD and HP-γ-CyD is straightforward and does not require a carrier polymeric matrix.[40] Also, both β-CyD/derivatives and γ-CyD/derivatives form inclusion complexes with α-LA.[10,15−17] α-LA is poorly water-soluble, yet, it becomes water-soluble by inclusion complexation with cyclodextrins.[16,17] Therefore, we are able to perform electrospinning of α-LA/cyclodextrin inclusion complex from its aqueous solutions. Most of the bioactive agents are hydrophobic and poorly water-insoluble, so, the use of some organic solvents and acids is required to dissolve the bioactive agents for the electrospinning process in order to encapsulate such bioactive agents into electrospun nanofibers.[20] However, the use of organic solvents and acids for the process is always a serious environmental issue, more importantly; the presence of toxic solvent residue in electrospun nanofibers would be a severe concern especially for the food related applications[20,41] Hence, the use of water for the electrospinning of cyclodextrin inclusion complex systems offers great advantage, especially for food applications.[31,32,38] Here, the electrospinning of aqueous solutions of both α-LA/HP-β-CyD and α-LA/HP-γ-CyD inclusion complex systems was successful and uniform α-LA/CyD nanofibers in the form of nanofibrous webs were produced. The detailed structural characterizations and the release, solubility, dissolution, and disintegration profile of α-LA/CyD nanofibrous webs were studied. The thermal stability and the antioxidant properties of α-LA/HP-β-CyD and α-LA/HP-γ-CyD nanofibrous webs were also evaluated.

MATERIALS AND METHODS

Materials. HP-β-CyD (Cavasol W7 HP, DS: ∼0.9, M_w = 1500 g/mol) and HP-γ-CyD (Cavasol W8 HP Pharma, DS: ∼0.6, M_w = 1540 g/mol) were donated by Wacker Chemie AG (U.S.A.). α-Lipoic acid [(α-LA), 98%, Alfa Aesar], deuterated dimethyl sulfoxide [(d_6-DMSO), 99.8%, Cambridge Isotope], phosphate buffered saline tablet (PBS, Sigma-Aldrich), 2,2′-azino-bis(3-ethylbenzothiazoline-6-sulfonic acid) (ABTS powder, Alfa Aesar), potassium persulfate [($K_2S_2O_8$), 99%, Acros Organics], sodium phosphate dibasic heptahydrate [(Na_2HPO_4), 98.0−102.0%, Fisher Chemical], potassium phosphate monobasic [(KH_2PO_4), ≥99.0%, Fisher Chemical], sodium chloride [(NaCl), >99%, Sigma-Aldrich], and o-phosphoric acid (85% (HPLC), Fisher Chemical) were obtained commercially. All of the materials were used without a further purification. Distilled water from Millipore system was used.

Electrospinning of CyD and α-LA/CyD Inclusion Complex Nanofibers. First, HP-β-CyD and HP-γ-CyD having 200% (w/v) solid concentration was dissolved in water. Afterward, α-lipoic acid (α-LA) was added to the clear HP-β-CyD and HP-γ-CyD solutions,

DOI: 10.1021/acs.jafc.9b05580
J. Agric. Food Chem. XXXX, XXX, XXX−XXX

separately to get 1/1 and 2/1, α-LA/CyD molar ratios for each CyD types. The inclusion complex formation between α-LA and CyD was achieved by stirring all α-LA/CyD aqueous systems for 24 h at room temperature. While α-LA/HP-β-CyD (1/1) system became clear, α-LA/HP-β-CyD (2/1), α-LA/HP-γ-CyD (1/1), and α-LA/HP-γ-CyD (2/1) systems became turbid by the end of 24 h. For the comparative characterizations, pristine HP-β-CyD and HP-γ-CyD nanofibers were produced, as well. The HP-β-CyD and HP-γ-CyD were electrospun into uniform and bead-free nanofibers using 200% (w/v) concentrated aqueous solutions of both CyD types.

The electrospinning equipment (Okyay Tech, model: SG10, Turkey) was used for the nanofiber production. The CyD and α-LA/CyD systems were loaded in 1 mL syringes, separately. The 27 or 23 G metal needle was fixed to the loaded syringes of CyD, α-LA/CyD (1/1) and α-LA/CyD (2/1) systems and constant flow rate (0.5 mL/h) was applied during the electrospinning process. A constant 15 kV was applied for the electrospinning process and the nanofibers in the form of nanofibrous webs were deposited on the grounded stationary metal plate. The collector was wrapped with a piece of aluminum foil and located at 15 cm far from the tip of the needle. The temperature and humidity was recorded as ∼20 °C and ∼55%, respectively during the electrospinning process.

Characterization and Measurements. *Morphological Analysis.* The morphological analyses of pristine HP-β-CyD, pristine HP-γ-CyD, α-LA/HP-β-CyD (1/1 and 2/1), and α-LA/HP-γ-CyD (1/1 and 2/1) nanofibers (NF) were performed by using scanning electron microscopy (SEM, Tescan-MIRA3). The CyD based nanofibers are nonconducting and therefore have charging problem during the SEM imaging, so each nanofibrous web which was fixed onto SEM stub was coated with thin layer of Au/Pd to enhance their conductivity for a better SEM imaging. For SEM imaging, the working distance and accelerating voltage were set to 10 mm and 10 kV, respectively. The average fiber diameter (AFD) was calculated with ImageJ software by measuring ∼100 fibers from different parts of SEM images.

Solution Properties. The conductivity of the HP-β-CyD, HP-γ-CyD, α-LA/HP-β-CyD (1/1 and 2/1) and α-LA/HP-γ-CyD (1/1 and 2/1) solutions was measured by using conductivitymeter (FiveEasy, Mettler Toledo) at 21−22 °C. The rheometer (AR 2000 rheometer, TA Instrument) was used to measure the viscosity of the α-LA/CyD solutions at 22 °C by using cone/plate accessory (CP 20-4 spindle type, 4°) at shear rate of 0.01−1000 s^{-1}.

^{1}H NMR Analyses. For the calculation of molar ratio between α-LA and CyD in α-LA/HP-β-CyD NF and α-LA/HP-γ-CyD NF, nuclear magnetic resonance spectrometer (NMR, Bruker AV500 with autosampler) was used and the data were recorded at 25 °C. For proton nuclear magnetic resonance (^{1}H NMR) measurements, α-LA powder, HP-β-CyD NF, HP-γ-CyD NF, α-LA/HP-β-CyD NF, and α-LA/HP-γ-CyD NF were dissolved in d_6-DMSO at the 40 g/L sample concentration, separately. The ^{1}H NMR spectra of each sample were recorded upon 16 scans and software (Mestranova) was utilized to integrate the chemical shifts (δ, ppm) for each sample. For the calculation of the molar ratio of α-LA/HP-β-CyD NF and α-LA/HP-γ-CyD NF, $-CH_3$ peak of CyD at 1.03 ppm and protons of α-LA assigned between 1.00 and 2.50 ppm were considered.

XRD Analyses. X-ray diffraction (XRD) data of α-LA powder, HP-β-CyD NF, HP-γ-CyD NF, α-LA/HP-β-CyD NF and α-LA/HP-γ-CyD were investigated by using X-ray diffractometer (Bruker D8 Advance ECO). The 40 kV and 25 mA were set and the XRD analyses were performed between the 2Θ angles of 5° and 30° by applying Cu Kα radiation.

FTIR Analyses. Attenuated total reflectance Fourier transform infrared spectrometer (ATR-FTIR, PerkinElmer, U.S.A.) was used to record the FTIR spectra of α-LA powder, HP-β-CyD NF, HP-γ-CyD NF, α-LA/HP-β-CyD NF, and α-LA/HP-γ-CyD NF. The FTIR spectra were recorded at a resolution of 4 cm^{-1} between 4000 and 600 cm^{-1} and 64 scans were collected.

Thermal Behavior Analyses. Differential scanning calorimeter (DSC, Q2000, TA Instruments, U.S.A.) and thermogravimetric analyzer (TGA, Q500, TA Instruments, U.S.A.) were used for the examination of thermal behavior of the samples. The DSC measurements were performed at a flow rate of 10 °C/min from 0 to 240 °C under N_2 atmosphere. In case of TGA measurements, the samples were heated from 25 to 600 °C with 20 °C/min heating rate under inert N_2 atmosphere.

Phase Solubility Analyses. Phase solubility analysis of α-LA was performed according to method of Higuchi and Conners.[42] The amount of α-LA above its solubility, HP-β-CyD and HP-γ-CyD powder with increasing concentrations (0−12 mM) were weighted into glass vials separately, and then water (5 mL) was added to each of these vials. The sealed vials were shielded from the light, and shaken at 25 °C under 450 rpm for 24 h by using incubator shaker. To remove the undissolved part of α-LA from the suspensions, they were filtered with 0.45 μm PTFE filter. The UV−vis spectrophotometry (Lambda 35, PerkinElmer) was used to calculate the specific amount of α-LA dissolved in filtered aliquots. The absorbance intensity at 335 nm was considered for the calculation of each α-LA/CyD system. The triple measurement average was considered to plot the phase solubility diagrams. The binding constant (K_s) was calculated from the following equation;

$$K_s = \frac{\text{slope}}{S_0(1 - \text{slope})}$$

where S_0 is the intrinsic solubility of α-LA in the absence of CyD.

In Vitro Release Test. The time dependent release profiles of α-LA/HP-β-CyD and α-LA/HP-γ-CyD nanofibrous webs (∼100 mg) were examined in distilled water (40 mL). The α-LA powder (∼12 mg) having the theoretical α-LA content in α-LA/HP-β-CyD was also evaluated for the comparison. First, α-LA/CyD nanofibrous web samples and α-LA powder were weighed and put into beaker separately and then distilled water was poured into each beaker. All aqueous solutions were shaken with the speed of 200 rpm at room temperature. The 0.5 mL aliquot was withdrawn, and an equal amount of fresh water was put in the medium again at the definite time points. The UV−vis spectrophotometer was used in order to analyze the dissolved concentration (μg/mL) of α-LA in the medium by considering the absorbance intensity at the wavelength of 335 nm. The calibration curve of α-LA showed acceptability with $R^2 \geq 0.99$ and was used to convert the absorbance values of measurement to concentration (μg/mL). The release test was performed in triplicate for each sample and results were reported as average.

Solubility and Thermal Stability Analyses. The solubility enhancement of α-LA encapsulated in α-LA/HP-β-CyD NF and α-LA/HP-γ-CyD NF was confirmed by UV−vis spectroscopy. Here, α-LA powder (∼4 mg) and α-LA/HP-β-CyD NF (∼33 mg) and α-LA/HP-γ-CyD NF (∼40 mg) web that include the same amount of α-LA was placed in distilled water (5 mL) and stirred for 24 h at 150 rpm. The undissolved part of α-LA in the solutions (if any present) was removed by 0.45 μm PTFE filter and the UV−vis measurements were performed between 280 and 460 nm. To examine the thermal stability of pure α-LA and α-LA in α-LA/CyD NF webs, all samples were weighted into glass vials as in solubility test, and kept at 100 °C oven for 24 h. Afterward, 5 mL of distilled water was added each vial and stirred for 24 h at 150 rpm. Each solution was filtered using 0.45 μm PTFE filter and UV−vis measurements were performed to evaluate the heat treated samples.

Dissolution and Disintegration Tests. For the dissolution test, α-LA (∼2.5 mg), α-LA/HP-β-CyD NF (∼20 mg), and α-LA/HP-γ-CyD NF (∼25 mg) NF web having the equal amount of α-LA were put into glass vials. For comparison, the pristine HP-β-CyD NF web (∼20 mg) and HP-γ-CyD NF web (∼25 mg) were also weighted and placed into glass vial. Then, 3 mL of distilled water was added into vials and video was recorded simultaneously to monitor the dissolution test. The disintegration behavior of α-LA/HP-β-CyD NF and α-LA/HP-γ-CyD NF web was investigated under the physiological condition in which the surface of a moist tongue was simulated.[43] For this purpose, a filter paper having correct size was placed in Petri dish (10 cm), then, it was wetted with artificial saliva (10 mL of aqueous mixture of 16.8 mM Na_2HPO_4, 1.4 mM KH_2PO_4 and 137 mM NaCl was prepared and pH was adjusted to 6.8 by

DOI: 10.1021/acs.jafc.9b05580
J. Agric. Food Chem. XXXX, XXX, XXX−XXX

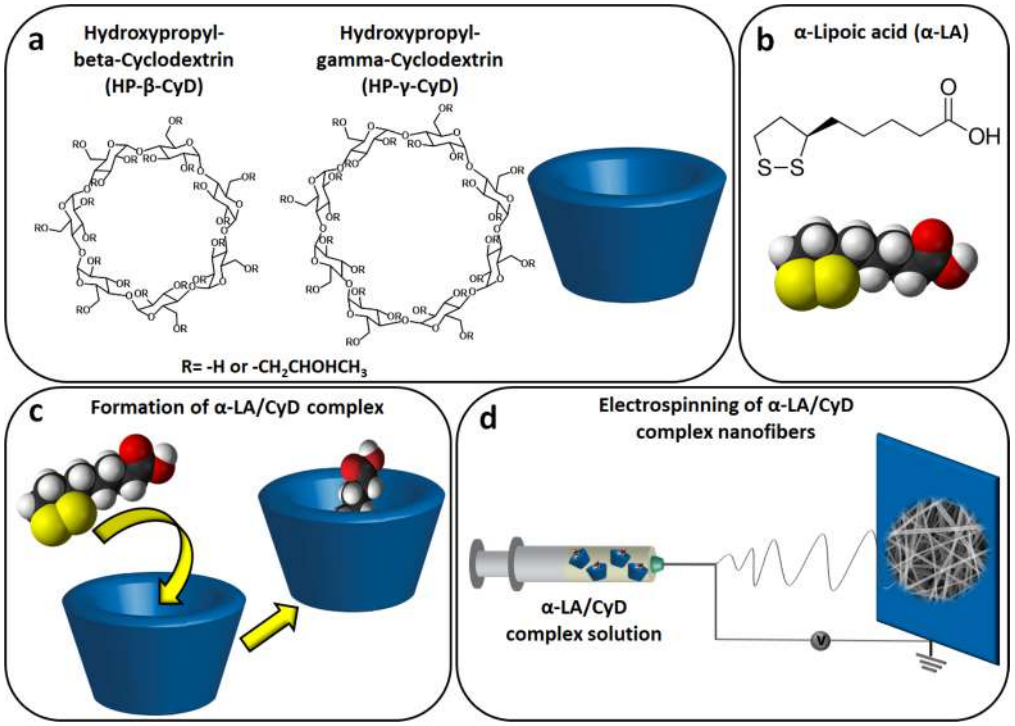

Figure 1. Chemical structure of (a) HP-β-CyD and HP-γ-CyD and (b) α-LA. (c) The illustration of inclusion complexation between α-LA and CyD, (d) electrospinning process for α-LA/CyD nanofibers.

phosphoric acid). Then, the excess artificial saliva was drained away from the Petri dish and a piece of α-LA/HP-β-CyD NF and α-LA/HP-γ-CyD NF webs were put at the center of the filter paper. The disintegration of α-LA/HP-β-CyD NF and α-LA/HP-γ-CyD NF webs was recorded as videos.

Antioxidant Activity Analyses. The antioxidant property of the samples was evaluated by ABTS (2,2′-azinobis (3-ethyl-benzothiazoline-6-sulfonate)) radical cation scavenging assay. First, the radical cation of $ABTS^{\bullet+}$ was generated by mixing aqueous solutions of ABTS (2.3 mM) and potassium persulfate (9.9 mM) at the volume ratio of 1/1 (v/v). Prior the experiment, the mixture was incubated at room temperature for 16 h by shielding from the light sources. Then, the $ABTS^{\bullet+}$ solution was diluted with phosphate buffer saline (PBS; pH 7.4) to make the reference absorbance (734 nm) intensity around 0.70. Then 3 mL of diluted solutions of $ABTS^{\bullet+}$ was added to the vials which contain α-LA powder (~2.5 mg), α-LA/HP-β-CyD NF (~20 mg) and α-LA/HP-γ-CyD NF (~20 mg) webs, separately. The time dependent UV−vis measurements were performed for each sample at 280−800 nm range. The decrease of the absorbance intensity at 734 nm was considered for the calculations of antioxidant performance. As control, the absorbance of the diluted stock solution and the inhibition profile of pristine CyD NF webs was also measured for 60 min period of time. The percentage of inhibition was calculated by the following equation:

$$\%\text{inhibition} = \frac{A_c - A_t}{A_c} \times 100$$

where A_c is the absorbance of control and A_t is the absorbance of the test sample. The mean values were obtained from triplicate experiments. The antioxidant property of the heat treated samples was further examined. For this, α-LA powder (~2.5 mg), α-LA/HP-β-CyD NF (~20 mg) and α-LA/HP-γ-CyD NF (~20 mg) webs located into glass vials were kept at 100 °C oven for 24 h. Then, 3 mL of the diluted solutions of $ABTS^{\bullet+}$ was added to these vials, and UV−vis spectra of each samples were recorded after 60 min incubation.

RESULTS AND DISCUSSION

Electrospinning of Nanofibers. The aqueous solutions of both α-LA/HP-β-CyD and α-LA/HP-γ-CyD inclusion complex systems were prepared by using highly concentrated CyD (200%, w/v) solutions (Figure 1). It is worth mentioning that such a highly concentrated CyD (200%, w/v) solution is mostly necessary in order to perform electrospinning of uniform nanofibers from CyD based systems without using polymeric carrier.[40,44] The HP-β-CyD and HP-γ-CyD are highly water-soluble, so, their 200% (w/v) concentrated aqueous solutions are clear and homogeneous showing that such high amount of HP-β-CyD and HP-γ-CyD can be dissolved in water for the preparation of the electrospinning solutions (Figure 2a-i, b-i).[40] α-LA is a poorly water-soluble molecule; yet, it becomes water-soluble by inclusion complexation with both HP-β-CyD and HP-γ-CyD. The α-LA/HP-β-CyD (1/1) aqueous solution was homogeneous signifying that α-LA becomes completely water-soluble by inclusion complexation with HP-β-CyD (Figure 2a-ii). The α-LA/HP-γ-CyD aqueous solution having 1/1 molar ratio was a bit turbid which may be due to the presence of a small amount of undissolved α-LA part in the α-LA/HP-γ-CyD system (Figure 2b-ii). However, α-LA also became mostly soluble in α-LA/HP-γ-CyD solution by inclusion complexation with HP-γ-CyD. We have also prepared 2/1 molar ratio of α-LA/CyD aqueous solutions in order to increase the amount of α-LA in the α-LA/CyD inclusion complex nanofibers. Both α-LA/HP-β-CyD and α-LA/HP-γ-CyD aqueous solutions having 2/1 molar ratio were quite turbid indicating that α-LA could not be completely dissolved at 2/1 molar ratio (Figure 2a-iii, b-iii). So, a molar ratio of 1/1 (α-LA/CyD) can be considered as the optimal molar ratio for inclusion complexation between α-LA and HP-β-CyD or HP-γ-CyD in this experimented conditions and concentration. Nonetheless, we have performed electrospin-

DOI: 10.1021/acs.jafc.9b05580
J. Agric. Food Chem. XXXX, XXX, XXX−XXX

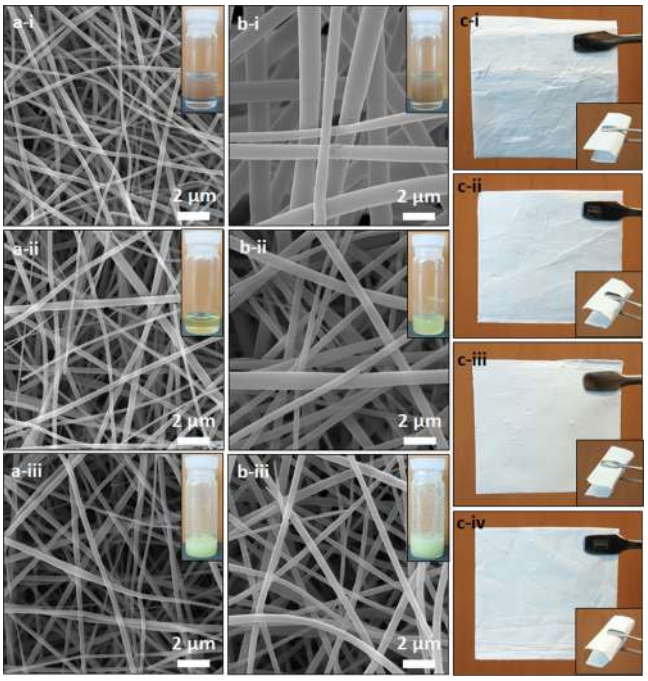

Figure 2. SEM images and the photographs (inset) of electrospinning solutions of (a-i) HP-β-CyD NF, (a-ii) α-LA/HP-β-CyD (1/1) NF, (a-iii) α-LA/HP-β-CyD (2/1) NF, (b-i) HP-γ-CyD NF, (b-ii) α-LA/HP-γ-CyD (1/1) NF, and (b-iii) α-LA/HP-γ-CyD (2/1) NF. The photographs of the resulting electrospun nanofibrous webs of (c-i) HP-β-CyD, (c-ii) HP-γ-CyD, (c-iii) α-LA/HP-β-CyD (1/1), and (c-iv) α-LA/HP-γ-CyD (1/1) systems.

ning for α-LA/HP-β-CyD (1/1 and 2/1) and α-LA/HP-γ-CyD (1/1 and 2/1) aqueous solutions. For comparative studies, electrospinning of pristine HP-β-CyD and HP-γ-CyD aqueous solutions having same concentration (200%, w/v) without containing α-LA was also performed. The electrospinning of all the α-LA/HP-β-CyD (1/1 and 2/1) and α-LA/HP-γ-CyD (1/1 and 2/1) systems were quite successful yielding bead-free nanofibers. Even though α-LA/HP-β-CyD (2/1) and α-LA/HP-γ-CyD (2/1) systems were containing some undissolved α-LA, bead-free and uniform nanofibers were able to electrospun from these aqueous solutions as well.

The SEM images show the morphology of the electrospun nanofibers (NF) of α-LA/HP-β-CyD (1/1 and 2/1) and α-LA/HP-γ-CyD (1/1 and 2/1), and the pristine HP-β-CyD and HP-γ-CyD (Figure 2). Table 1 summarizes the solution composition and properties (viscosity and conductivity) and the average fiber dimeter (AFD) of the electrospun samples. The pristine HP-β-CyD NF and HP-γ-CyD NF have AFD of 220 ± 60 nm and 1260 ± 245 nm, respectively. The AFD of HP-β-CyD NF is much smaller than the AFD of HP-γ-CyD NF since HP-β-CyD aqueous solution has significantly lower viscosity and higher conductivity than HP-γ-CyD aqueous solution, therefore, electrospinning resulted in much thinner fibers for HP-β-CyD NF due to more stretching of the jet.[40,45] The addition of α-LA in HP-β-CyD and HP-γ-CyD aqueous solutions lowered the viscosity but increased the conductivity of the solutions. The α-LA/HP-β-CyD (1/1) and α-LA/HP-γ-CyD (1/1) aqueous solutions have lower viscosity but higher conductivity than their corresponding 2/1 aqueous solutions. Yet, the AFD of both α-LA/HP-β-CyD (1/1) NF and α-LA/HP-β-CyD (2/1) NF was very similar having 235 ± 90 nm and 230 ± 90 nm, respectively. Similarly, The AFD of both α-LA/HP-γ-CyD (1/1) NF and α-LA/HP-γ-CyD (2/1) NF was also very close to each other having 450 ± 180 and 425 ± 150 nm, respectively. The α-LA/HP-β-CyD NF (1/1 and 2/1) yielded thinner fibers than α-LA/HP-γ-CyD NF (1/1 and 2/1), since α-LA/HP-β-CyD (1/1 and 2/1) solutions have lower viscosity and higher conductivity than α-LA/HP-γ-CyD (1/1 and 2/1) solutions.

It is also worth to mention that the electrospinning process was somewhat not very stable and the nanofiber production yield was less for α-LA/HP-β-CyD (2/1) and α-LA/HP-γ-CyD (2/1) systems when compared to electrospinning of α-LA/HP-β-CyD (1/1) and α-LA/HP-γ-CyD (1/1) systems. Even we used the same electrospinning parameters and same process time for the production of fibers, only α-LA/HP-β-CyD (1/1) and α-LA/HP-γ-CyD (1/1) systems resulted in high amount of nanofibers which we could obtain self-standing nanofibrous webs (Figure 2). In the case of α-LA/CyD (2/1) systems, the fiber yield was low, and therefore we could not obtain self-standing nanofibrous webs under the same electrospinning process time as α-LA/CyD (1/1) systems. Therefore, α-LA/HP-β-CyD NF and α-LA/HP-γ-CyD NF prepared with (1/1) molar ratio were selected for further characterizations and testing as discussed in the upcoming sections.

Structural Characterization. ^{1}H NMR analyses were performed in order to calculate the molar ratio between α-LA and CyD in α-LA/HP-β-CyD NF and α-LA/HP-γ-CyD NF samples. The initial molar ratio of the electrospinning solutions of α-LA/HP-β-CyD and α-LA/HP-γ-CyD was 1/1 (α-LA/CyD) which corresponds to ~12% (w/w) of α-LA content in electrospun α-LA/CyD NF samples, however, there may be some loss of α-LA during the electrospinning process. The ^{1}H NMR spectra of pure α-LA, pristine HP-β-CyD NF and HP-γ-CyD NF, α-LA/HP-β-CyD NF and α-LA/HP-γ-CyD NF dissolved in d_6-DMSO are given Figure 3. The molar ratio between α-LA and CyD was determined by integrating the proportion of the specific peaks of α-LA and CyD in α-LA/HP-β-CyD NF and α-LA/HP-γ-CyD NF samples. The protons of $-CH_3$ group (1.03 ppm) in modified CyDs (HP-β-CyD and HP-γ-CyD) and the α-LA peaks between 1.00 and 2.50 ppm[46] which are not overlapped with CyD were used for the

Table 1. Solution Properties CyD and α-LA/CyD Systems and the Fiber Diameters of CyD and α-LA/CyD Nanofibers

sample	molar ratio (α-LA/CyD)	viscosity (Pa·s)	conductivity (μS/cm)	average fiber diameter (nm)
HP-β-CyD		1.533	36.3	220 ± 60
α-LA/HP-β-CyD (1/1)	1/1	0.873	49.1	235 ± 90
α-LA/HP-β-CyD (2/1)	2/1	1.248	39.0	230 ± 90
HP-γ-CyD		2.567	5.8	1260 ± 245
α-LA/HP-γ-CyD (1/1)	1/1	1.935	9.9	450 ± 180
α-LA/HP-γ-CyD (2/1)	2/1	2.396	8.6	425 ± 150

DOI: 10.1021/acs.jafc.9b05580
J. Agric. Food Chem. XXXX, XXX, XXX−XXX

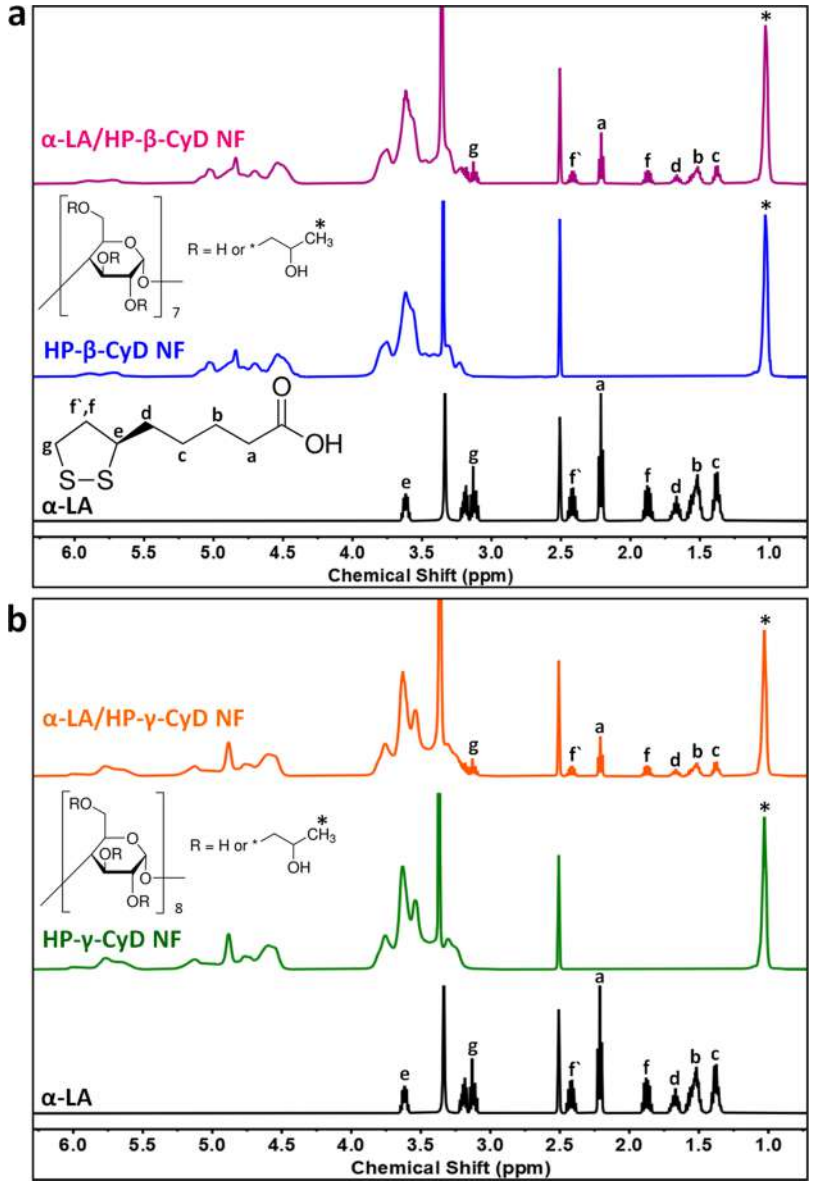

Figure 3. ^{1}H NMR spectra of (a) α-LA, HP-β-CyD NF, and α-LA/HP-β-CyD NF and (b) α-LA, HP-γ-CyD NF and α-LA/HP-γ-CyD NF. The ^{1}H NMR spectra were recorded by dissolving the samples in d_6-DMSO.

calculation of molar ratio in these samples. From the ^{1}H NMR peak integrations, the molar ratio of α-LA/CyD was calculated as ~1/1 and ~0.85/1 for α-LA/HP-β-CyD NF and α-LA/HP-γ-CyD NF, respectively. The ^{1}H NMR analyses revealed that the encapsulation of α-LA was very efficiency during the electrospinning process and the initial molar ratio of 1/1 was totally preserved for α-LA/HP-β-CyD NF and most of the α-LA was preserved for α-LA/HP-γ-CyD NF sample. For α-LA/HP-γ-CyD NF, the molar ratio of α-LA/CyD is slightly lower (~0.85/1) than the initial ratio of 1/1. In brief, α-LA/CyD NF was successfully produced by the loading capacity of ~12% (w/w) and ~10% (w/w), so, the encapsulation efficiency of ~100% and ~85% for α-LA/HP-β-CyD NF and α-LA/HP-γ-CyD NF was achieved, respectively. The reason for the somewhat lower encapsulation efficiency of α-LA/HP-γ-CyD NF might be the presence of a small amount of uncomplexed α-LA part in α-LA/HP-γ-CyD NF (Figure 2b-ii) which could not be effectively included within the HP-γ-CyD matrix during the electrospinning process. It is also noteworthy to mention that the ^{1}H NMR spectra of α-LA/HP-β-CyD NF and α-LA/HP-γ-CyD NF have the same peaks of pure α-LA and pristine CyD elucidating that α-LA was structurally protected during the electrospinning process. The stabilization of α-LA within CyD inclusion complex nanofibers is important for its antioxidant activity as we studied and discussed in the below sections.

The state of inclusion complexation between α-LA and CyDs (HP-β-CyD and HP-γ-CyD) in α-LA/HP-β-CyD NF and α-LA/HP-γ-CyD NF was confirmed by XRD. The XRD technique provides valuable information for the characterization of the CyD inclusion complexes.[47,48] When complete inclusion complexation is achieved, guest molecules are reside within the CyD cavities and therefore cannot form crystallites since they are separated from each other by the CyD molecules. In the case of uncomplexed state, it is likely that guest molecules are segregated from CyD molecules and form crystalline aggregates. α-LA is a crystalline molecule which has distinctive XRD peaks at 23.5°, 24.1°, and 28.8° (Figure 4a).[17]

DOI: 10.1021/acs.jafc.9b05580
J. Agric. Food Chem. XXXX, XXX, XXX−XXX

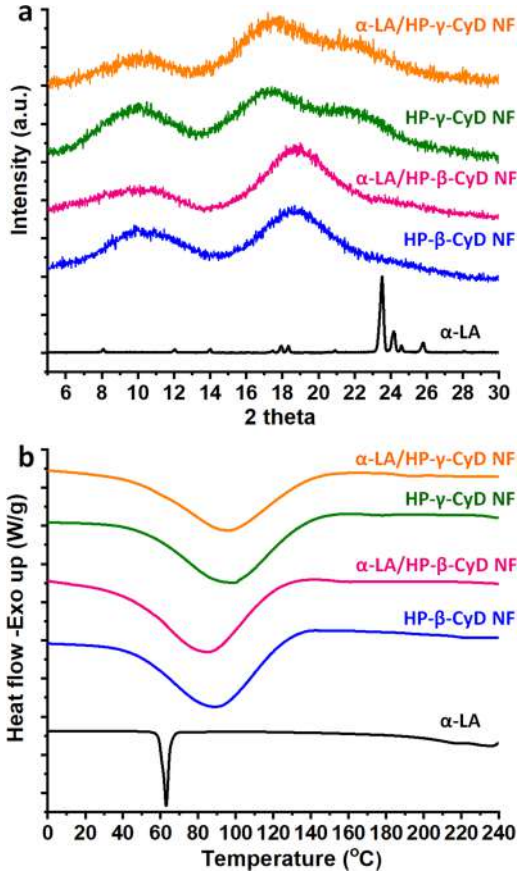

Figure 4. (a) XRD patterns and (b) DSC thermograms of α-LA, HP-β-CyD NF, α-LA/HP-β-CyD NF, HP-γ-CyD NF, and α-LA/HP-γ-CyD NF.

HP-β-CyD and HP-γ-CyD are both amorphous CyD types; hence, the XRD patterns of pristine HP-β-CyD NF and HP-γ-CyD NF have broad halo without any significant diffraction peaks. The XRD patterns of α-LA/HP-β-CyD NF and α-LA/HP-γ-CyD NF were very similar to that of pristine HP-β-CyD NF and HP-γ-CyD NF samples showing broad diffraction pattern. The XRD patterns of α-LA/HP-β-CyD NF and α-LA/HP-γ-CyD NF did not have any specific diffraction peaks for crystalline α-LA elucidating that α-LA molecules are in the state of inclusion complexed with each type of the CyD (HP-β-CyD and HP-γ-CyD). So, α-LA molecules are in amorphous phase without forming any crystalline aggregates in α-LA/HP-β-CyD NF and α-LA/HP-γ-CyD NF samples. In another related study reported by Maeda et al., the solid complexes of α-LA and modified CyD of sulfobutylether-beta-cyclodextrin (SBE-β-CD) also indicated amorphous XRD pattern upon the inclusion complexation and complete disappearance of the characteristic peaks of α-LA.[17] For α-LA/HP-γ-CyD solution, a few amount of uncomplexed α-LA was present, yet, α-LA/HP-γ-CyD NF did not have XRD pattern for any crystalline α-LA indicating that even if there was few amount of uncomplexed/undissloved α-LA in this sample, the α-LA was totally in the amorphous state. It is also worth to mention that the amorphous state of α-LA and its inclusion complexation with CyD would facilitate its fast-dissolution in α-LA/CyD NF samples as seen in the dissolution tests that is discussed in detail in the upcoming sections.

DSC technique can provide valuable evidence for the inclusion complexation state between host CyD molecules and guest molecules.[48] For example, guest molecules cannot form crystalline aggregates since they are segregated from each other by the cavity of CyD molecules; hence, there will be no melting point observed for the guest molecule for the inclusion

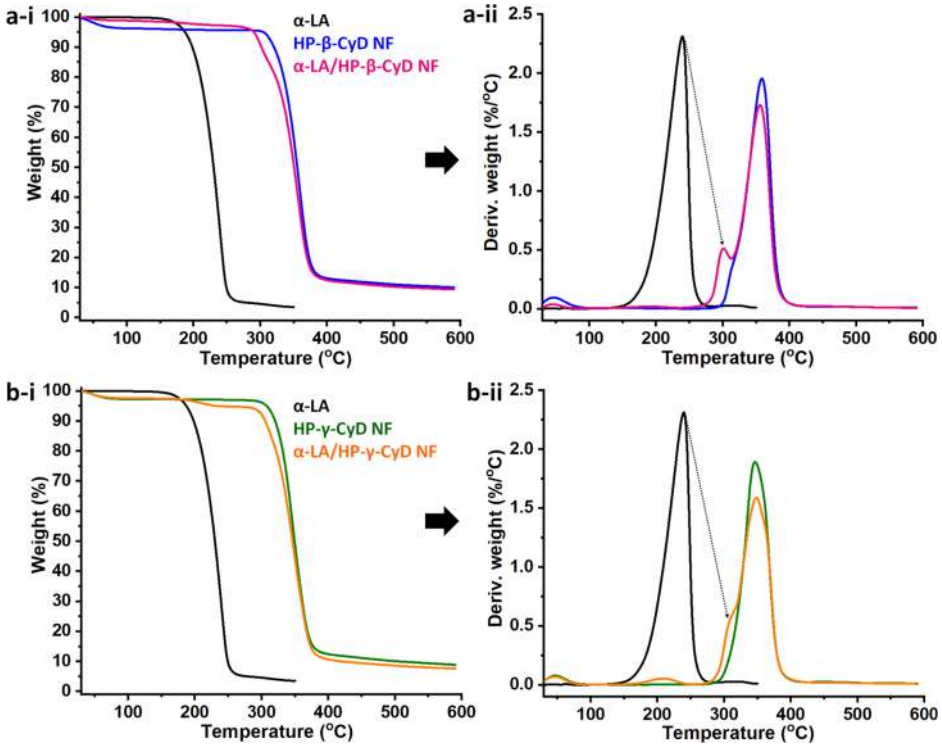

Figure 5. TGA thermograms and derivates of (a-i,ii) α-LA, HP-β-CyD NF, and α-LA/HP-β-CyD NF and (b-i,ii) α-LA, HP-γ-CyD NF, and α-LA/HP-γ-CyD NF.

DOI: 10.1021/acs.jafc.9b05580
J. Agric. Food Chem. XXXX, XXX, XXX−XXX

complexes.[48] Figure 4b displays the DSC thermograms of the pure α-LA powder, pristine HP-β-CyD NF and HP-γ-CyD NF samples, and the α-LA/HP-β-CyD NF and α-LA/HP-γ-CyD NF samples. The pure α-LA has a crystalline nature having a distinct melting point at 63 °C.[17] The pristine HP-β-CyD and HP-γ-CyD are amorphous CyD types, so, there is no melting point for HP-β-CyD NF and HP-γ-CyD NF,[40] and the DSC thermograms of HP-β-CyD NF and HP-γ-CyD NF samples have only broad endothermic peak between ∼30−140 °C because of the water loss.[49] The DSC data of α-LA/HP-β-CyD NF and α-LA/HP-γ-CyD NF were similar to that of their pristine HP-β-CyD NF and HP-γ-CyD NF samples having very broad endothermic peak between the ranges of 30−140 °C due to water loss. Both α-LA/HP-β-CyD NF and α-LA/HP-γ-CyD NF have not shown any melting point for α-LA signifying that α-LA molecules are inclusion complexed with CyD and therefore they are not in the crystalline form. Our finding is also correlated with the previous reports in which the melting point of α-LA was disappeared as a result of inclusion complexation with different kinds of CyD and derivates.[10,15−17,46] In brief, the DSC data are in good agreement with XRD data revealing that α-LA molecules were in the amorphous state in both of α-LA/HP-β-CyD NF and α-LA/HP-γ-CyD NF samples due to inclusion complexation with CyD.

The TGA thermograms of the pure α-LA powder, pristine HP-β-CyD NF and HP-γ-CyD NF samples, and α-LA/HP-β-CyD NF and α-LA/HP-γ-CyD NF samples are shown in Figure 5. The pure α-LA has shown one-step main degradation which occurs between 130 and 285 °C. The pristine HP-β-CyD NF and HP-γ-CyD NF samples have initial weight (%) loss below 100 °C which correspond to evaporation of water.[40] The main thermal degradation of pristine HP-β-CyD NF and HP-γ-CyD NF samples occurs between 280−430 and 265−420 °C, respectively. The TGA thermograms of α-LA/HP-β-CyD NF and α-LA/HP-γ-CyD NF have shown weight losses in multiple steps. Similar to pristine HP-β-CyD NF and HP-γ-CyD NF samples, α-LA/HP-β-CyD NF and α-LA/HP-γ-CyD NF also have shown weight loss below 100 °C due to evaporation of water present in these sample. The major weight loss due to the main degradation of CyD was observed between 255−430 °C and 260−420 °C for α-LA/HP-β-CyD NF and α-LA/HP-γ-CyD NF, respectively. The α-LA/HP-β-CyD NF and α-LA/HP-γ-CyD NF samples have also shown two different steps of weight loss for the degradation of α-LA present in these samples. The derivative weight (%) loss curve of α-LA/HP-β-CyD NF showed that there was a minor weight loss between 140 and 250 °C, and the major weight (%) loss peaked at about 300 °C due to degradation of α-LA. The derivative weight change curve of α-LA/HP-γ-CyD NF showed a similar pattern like α-LA/HP-β-CyD NF having two steps weight (%) loss for the thermal degradation of α-LA, the first weight loss step was between 140 and 250 °C and the later weight loss was peaked at about 300 °C. The weight percentage of the guest molecule in CyD inclusion complex systems can be calculated by the TGA data. However, the exact amount of α-LA in α-LA/HP-β-CyD NF and α-LA/HP-γ-CyD NF samples could not be calculated from these TGA data since the major weight loss step of α-LA at about 300 °C was overlapped with the main degradation of CyD. Nonetheless, the weight percentage of α-LA in α-LA/HP-β-CyD NF and α-LA/HP-γ-CyD NF samples was calculated by ^{1}H NMR as previously discussed, and the molar ratios of ∼1/1 and ∼0.85/1 correspond to ∼12.0% (w/w) and ∼10% (w/w) of α-LA in α-LA/HP-β-CyD NF and α-LA/HP-γ-CyD NF, respectively. On the other hand, the minor weight loss of α-LA at lower temperature (140−250 °C) was calculated as ∼1.5% (w/w) and ∼2.7% (w/w) for α-LA/HP-β-CyD NF and α-LA/HP-γ-CyD NF, respectively. This finding suggests that the interaction between α-LA and HP-β-CyD is stronger than the interaction between α-LA and HP-γ-CyD, because there is less amount of α-LA in α-LA/HP-β-CyD NF (∼1.5%, weight loss) compared to α-LA/HP-γ-CyD NF (∼2.7%, weight loss) which could not interact with CyD cavity or make weak interaction. Actually, the phase solubility tests also revealed that α-LA has a stronger binding with HP-β-CyD than HP-γ-CyD which was discussed in detail in the following section. So, the TGA data correlates with the phase solubility tests in which α-LA is thermally more stable in α-LA/HP-β-CyD NF due to stronger interaction with the HP-β-CyD when compared to α-LA/HP-γ-CyD NF. More importantly, when compared to pure α-LA, the α-LA has shown a higher temperature stability in α-LA/HP-β-CyD NF and α-LA/HP-γ-CyD NF samples due to inclusion complexation with CyD. The thermal stability enhancement for the guest molecule is typically observed for the CyD inclusion complexes.[48] The major weight loss step of α-LA that shifted up to 300 °C that proved the higher temperature stability of α-LA in α-LA/HP-β-CyD NF and α-LA/HP-γ-CyD NF samples (Figure 5a-ii, b-ii). In brief, TGA data provided strong evidence for the state of inclusion complexation between α-LA and both of the CyD (HP-β-CyD and HP-γ-CyD) in α-LA/CyD NF samples and revealed that the thermal stability of α-LA has increased in α-LA/CyD NF samples due to the inclusion complexation between α-LA and CyD.

The FTIR spectra of the pure α-LA powder, pristine HP-β-CyD NF, HP-γ-CyD NF, α-LA/HP-β-CyD NF, and α-LA/HP-γ-CyD NF are given in Figure 6. There would be molecular interactions between guest molecules and CyD in the case of inclusion complexation, and FTIR is a useful technique to study such molecular interactions since there would be some shift for the characteristic FTIR peaks of the guest molecules by these molecular interactions with CyD.[48] The α-LA has a characteristic absorption band at 1687 cm^{-1} due to the C═O stretching of the acid group.[17] The FTIR spectra of pristine HP-β-CyD NF and HP-γ-CyD NF have distinct absorption peaks at 3000−3600 cm^{-1}, 1020 and 1150 cm^{-1} corresponding to −OH groups, C−C/C−O stretching, and antisymmetric C−O−C glycosidic bridge stretching of CyD, respectively.[32] Due to the much higher weight percentage of CyD in α-LA/HP-β-CyD NF and α-LA/HP-γ-CyD NF, the characteristic peaks of α-LA are masked in the FTIR spectra of these samples. Yet, the C═O stretching of α-LA has also been recorded in the FTIR spectra of α-LA/HP-β-CyD NF and α-LA/HP-γ-CyD NF confirming its presence in these samples. More importantly, it was observed that the C═O peak shifted to higher wavenumber of 1712 cm^{-1} for α-LA/HP-β-CyD NF and α-LA/HP-γ-CyD NF due to molecular interactions and this further suggest that α-LA is inclusion complexed with CyD in both of these α-LA/CyD NF samples. Ikuta et al. and Racz et al. also reported a higher frequency shift for the carbonyl (C═O) peak of α-LA in case of inclusion complex of CyD and α-LA and attributed this observation to the interaction between CyD and α-LA existing in the complex formulation.[10,46]

DOI: 10.1021/acs.jafc.9b05580
J. Agric. Food Chem. XXXX, XXX, XXX−XXX

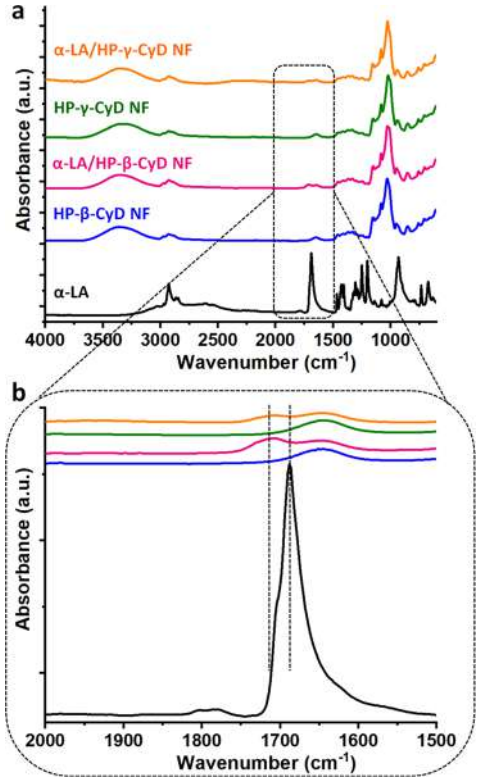

Figure 6. (a) The full and (b) expanded range FTIR spectra of α-LA, HP-β-CyD NF, HP-γ-CyD NF, α-LA/HP-β-CyD NF, and α-LA/HP-γ-CyD NF.

The phase solubility analysis is generally performed for determining the solubilizing effect of CyD on hydrophobic guest molecules. Additionally, the stability constant of CyD inclusion complex can be calculated by phase solubility diagrams.[6,50,51] Here, the α-LA/HP-β-CyD and α-LA/HP-γ-CyD solutions having different CyD concentrations were filtered and analyzed by UV−vis spectroscopy technique after 24 h stirring. Figure 7a shows the phase solubility diagrams which represent the solubility of α-LA against increasing CyD concentration (0 to 12 mM). Due to the inclusion complex formation, the solubility of α-LA was increased ∼3 and ∼2 times with 12 mM of HP-β-CyD and HP-γ-CyD, respectively. Various phase solubility diagrams can be observed depending on the guest molecules and CyD types.[42] For modified cyclodextrins, A-type phase solubility diagram is generally observed and has subtypes of A_L, A_N, and A_P which corresponds to the linear enhancement for the guest solubility against increasing CyD concentration, positive deviation of isotherms and negative deviation of isotherms, respectively.[42,51] In our system, the phase solubility diagrams show almost linear profile until the CyD concentration of 12 mM. The linear increase in the solubility of α-LA with increase CyD concentration reveals the tendency of forming 1/1 molar ratio inclusion complexes.[42] Here, the straight-line of phase solubility diagram enabled to calculate the apparent stability constant (K_s). K_s value, which fundamentally represents the binding strength between guest molecule and CyD, was calculated as 281 and 76 M^{-1} for α-LA/HP-β-CyD and α-LA/HP-γ-CyD systems, respectively. This finding suggests that there is a better size match between α-LA and HP-β-CyD cavity, so HP-β-CyD formed a more stable inclusion complex

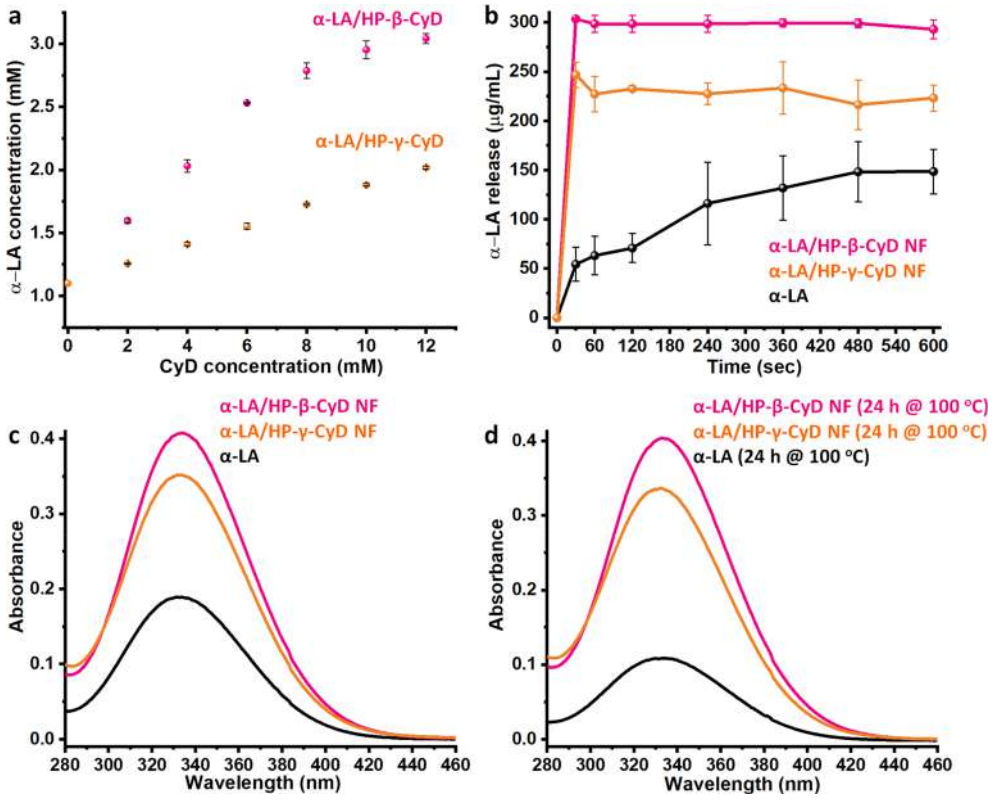

Figure 7. (a) Phase solubility diagram of α-LA/CyD systems. (b) Time dependent release profiles of α-LA, α-LA/HP-β-CyD NF, and α-LA/HP-γ-CyD NF. UV−vis spectra of aqueous solutions of (c) α-LA, α-LA/HP-β-CyD NF, and α-LA/HP-γ-CyD NF and (d) heat treated (100 °C for 24 h) α-LA, α-LA/HP-β-CyD NF, and α-LA/HP-γ-CyD NF.

DOI: 10.1021/acs.jafc.9b05580
J. Agric. Food Chem. XXXX, XXX, XXX−XXX

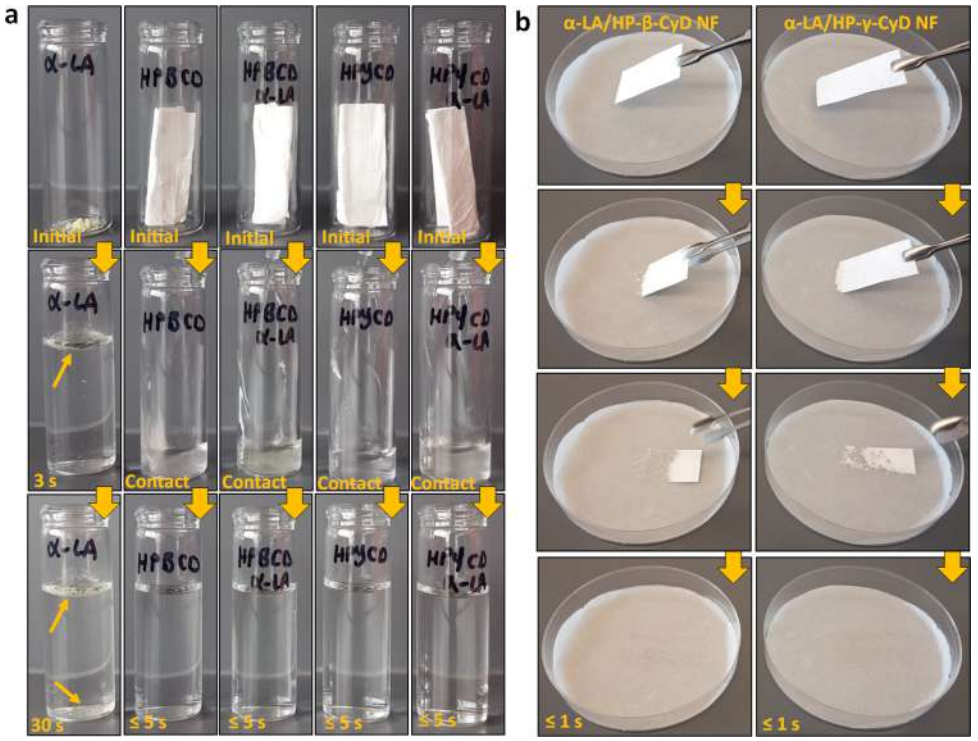

Figure 8. (a) The dissolution behavior of α-LA powder, HP-β-CyD NF, α-LA/HP-β-CyD NF, HP-γ-CyD NF, and α-LA/HP-γ-CyD NF webs in distilled water. (b) The disintegration behavior of α-LA/HP-β-CyD NF and α-LA/HP-γ-CyD NF webs when wetted with artificial saliva. The pictures were captured from Videos S1 and S2.

with α-LA compared to HP-γ-CyD. The bigger cavity size of HP-γ-CyD seems to be not as effective as HP-β-CyD for stabilizing the interaction with α-LA in the aqueous environment, therefore, less amount of α-LA was encapsulated in HP-γ-CyD and lower water solubility was observed compared to HP-β-CyD. Since HP-β-CyD formed stronger inclusion complexes with α-LA, higher amount of α-LA was encapsulated in α-LA/HP-β-CyD NF compared to α-LA/HP-γ-CyD NF as confirmed by ^{1}H NMR results. In another related study, Maeda et al. released the stability constant value of α-LA/HP-β-CyD system as 350 M^{-1} [17] and it is slightly different from the calculated value in this study (281 M^{-1}). As Loftsson et al. reported, the variation of the substitution degree of HP groups in HP-β-CyD might cause difference between the stability constant value for the same guest/CyD system, and the increasing substitution degree can decrease the binding strength between guest and HP-β-CyD.[52] The substitution degree of HP-β-CyD was not mentioned in the previous study;[17] however, we have determined the stability constant of 281 M^{-1} for the α-LA/HP-β-CyD system in which the HP-β-CyD we used has substitution degree of ~0.9.

Figure 7b depicted the in vitro release profile of α-LA from α-LA/CyD nanofibrous webs and α-LA powder. The α-LA/CyD nanofibrous webs dissolved instantly upon the contact with the water and α-LA/HP-β-CyD and α-LA/HP-γ-CyD nanofibrous webs released 303 ± 0.7 and 246 ± 12 μg/mL of α-LA in the first 30 s, respectively, and indicated plateau profile up to 10 min endorsing the fast-dissolution behavior of α-LA in α-LA/CyD nanofibrous webs. However, α-LA powder did not dissolve immediately and just 54 ± 17 μg/mL of α-LA was released into the dissolution medium in the first 30 s, then it reached up to 148 ± 22 μg/mL by the end of 10 min. The results confirmed the remarkable enhancement of the dissolution of α-LA in the α-LA/CyD nanofibrous webs compared to pure α-LA powder. The unique features of inclusion complex formation between α-LA and CyD; high water-solubility of HP-β-CyD and HP-γ-CyD; high surface area and highly porous structure of nanofibrous webs promoted the rapid release of α-LA from α-LA/CyD nanofibrous webs by providing an actual penetration path and influential contact sides for the dissolution media. As seen in Figure 7b, α-LA/CyD nanofibrous webs showed release of different amount of α-LA for the same sample amount (~100 mg) because of the different α-LA content in α-LA/CyD nanofibrous webs. This finding is well correlated with the encapsulation efficiency values of ~100% and ~85% for α-LA/HP-β-CyD NF and α-LA/HP-γ-CyD NF, respectively which were determined using ^{1}H NMR technique. To conclude, both α-LA/CyD nanofibrous webs provided an enhanced dissolution rate and release profile for α-LA due to the inclusion complexation and the nanofibrous structure of α-LA/CyD NF, and this revealed the noticeable potential of α-LA/CyD nanofibrous webs as fast-dissolving delivery system.

The solubility tests were performed to demonstrate the solubility enhancement of α-LA in α-LA/CyD NF compared to pure α-LA. For solubility test, α-LA/HP-β-CyD NF (~33 mg) and α-LA/HP-γ-CyD NF (~40 mg) including the same amount of α-LA (~4 mg) were dissolved in water for 24 h. Afterward, each solution was filtered to remove the undissolved α-LA if any present and UV−vis spectroscopy measurement was performed for the final aliquot. Figure 7c indicates the UV−vis spectra of the aqueous solution of α-LA, α-LA/HP-β-CyD NF, and α-LA/HP-γ-CyD NF. All solutions were prepared so as to include the same amount of α-LA (~4 mg), however the intensity of the α-LA/CyD NF solutions are higher than the α-LA solution. The result clearly showed that

DOI: 10.1021/acs.jafc.9b05580
J. Agric. Food Chem. XXXX, XXX, XXX−XXX

the water solubility of α-LA was enhanced in case of α-LA/CyD NF owing to inclusion complexation. As is seen in UV−vis spectra, α-LA/HP-γ-CyD NF have slightly lower intensity compared to α-LA/HP-β-CyD NF, because HP-γ-CyD has a lower solubility increase of α-LA (∼2 times) than the HP-β-CyD (∼3 times) as indicated by the phase solubility test. Additionally, there were smaller amounts of uncomplexed α-LA in the solution of α-LA/HP-γ-CyD which could not be dissolved and therefore filtered out, so that the intensity of the UV−vis spectrum is lower than the solution of α-LA/HP-β-CyD NF. As it was discussed in the phase solubility part, HP-β-CyD formed a more favorable inclusion complex with α-LA than HP-γ-CyD; therefore, a slightly lower encapsulation efficiency was observed in case of HP-γ-CyD. In addition, the higher viscosity of the HP-γ-CyD solution might be another drawback which makes it difficult to achieve 1/1 molar ratio inclusion complexation between α-LA and HP-γ-CyD.

As it was discussed in the previous sections, α-LA is moderately stable solid substance which suffers from the instability against thermal treatment.[16] On the other hand, the earlier studies showed that thermal stabilization of α-LA can be improved by encapsulation of α-LA into CyD cavities.[4,10,12,15−17] Here, UV−vis measurements were performed to examine the thermal stabilization of α-LA in α-LA/CyD NF. For this purpose, pure α-LA powder (∼4 mg) and α-LA/CyD NF webs having the same amount of α-LA were prepared as a solubility test and kept at 100 °C in an oven for 24 h. Then, all samples were mixed with water (5 mL), stirred for 24 h at room temperature and filtered before the UV−vis measurement. Figure 7d shows the UV−vis absorbance of the solution of the heat treated α-LA and α-LA/CyD NF webs. When UV−vis spectra of heat treated samples (Figure 7d) are compared with pristine ones (Figure 7c), there is no difference between the absorbance profiles of α-LA/CyD NF before and after heat treatment. However, the heat treatment induced considerable loss of pure α-LA by ∼42% reduction of absorbance intensity. In brief, α-LA/CyD NF webs can be quite effective in the stabilizing of α-LA against high temperature owing to inclusion complex formation. In addition, the very same UV−vis spectrum (Figure S1) was recorded for the α-LA/CyD NF samples stored for 2 months (55−65% RH and ∼22 °C) confirming the stability of the α-LA in α-LA/CyD NF under the long storage periods.

The fast-dissolution of α-LA/HP-β-CyD NF and α-LA/HP-γ-CyD NF webs was investigated with the pouring of 3 mL of water into the glass vials (Figure 8a, Video S1). In order to have the same amount of α-LA (∼2.5 mg) in α-LA/CyD NF webs, we placed ∼20 mg of α-LA/HP-β-CyD NF web and ∼25 mg of α-LA/HP-γ-CyD NF web into the vials, separately. For comparison, the same quantity of pure α-LA powder (∼2.5 mg) and pristine HP-β-CyD NF web (∼20 mg) and HP-γ-CyD NF web (∼25 mg) was also placed into a glass vial. α-LA powder did not dissolve with the addition of water because of its limited water solubility. The pristine HP-β-CyD and HP-γ-CyD NF webs were dissolved immediately upon contact with water due to high water solubility of modified CyD types of HP-β-CyD and HP-γ-CyD. Both α-LA/HP-β-CyD NF and α-LA/HP-γ-CyD NF webs also indicate fast-dissolving profile when water added to the vials. This result suggests the improved water solubility of α-LA in α-LA/CyD NF webs. On the other hand, while there was no indication of the undissolved α-LA in α-LA/HP-β-CyD NF web, there was very few undissolved α-LA parts observed in the vial of LA/HP-γ-CyD NF webs because of the uncomplexed α-LA content (Video S1). This finding also supports the dissolution test at which the solution of LA/HP-γ-CyD NF webs indicates lower UV absorbance intensity compared to α-LA/HP-β-CyD NF web, even both α-LA/CyD NF web include the same amount of α-LA.

The disintegration of α-LA/CyD NF webs was examined by using wet filter paper in order to simulate the moist environment of the oral cavity.[43] The disintegration behavior of α-LA/HP-β-CyD NF and α-LA/HP-γ-CyD NF webs was recorded in Video S2 and displayed in Figure 8b. Both α-LA/CyD NF webs were instantly dissolved by artificial saliva. The HP-β-CyD and HP-γ-CyD are highly water-soluble CyD types, so, HP-β-CyD and HP-γ-CyD being as nanofiber matrix facilitate the rapid disintegration and fast dissolution of the α-LA/CyD NF webs.[53] The high surface area and porous structure of nanofibrous web are other important properties which provide easy penetration for liquid for the disintegration and dissolution of nanofibers.[25] In conclusion, the nanofibrous structure of α-LA/CyD NF webs can ensure the easy penetration of saliva in the mouth, additionally inclusion complex formation between α-LA and CyD (HP-β-CyD and HP-γ-CyD) and the high water solubility of modified CyD can enable the instant release of α-LA upon fast-dissolution.

Reactive oxygen species (ROS) and free radicals can oxidize and/or react with various biomolecules (lipids, proteins, DNA etc.) and can cause or induce several human pathologies such as cancer, stroke, neurodegenerative diseases, etc.[54,55] Antioxidants are presumed to deactivate the destructive effects of ROS and free radicals by scavenging them.[55] α-LA is considered as a natural antioxidant which has a therapeutic action for the supplementary treatment of several diseases such as, cancer, diabetes, auto immune, cardiovascular, and neurodegenerative diseases.[2,3,56] The chemical reactivity and so the antioxidants potential of α-LA is derived from the dithiol ring in the structure and as it was reported in the previous studies, both oxidized (LA) and reduced (DHLA) forms of α-LA are capable of scavenging ROS (hydroxyl radicals, singlet oxygen, etc.) and free radicals, regenerating antioxidants (vitamins E and C), and possessing metal chelating.[1−3,54,56] Unfortunately, α-LA is poorly water-soluble and also a moderately stable compound that can polymerize/degrade above its melting point, or be damaged upon light exposure.[2] All these drawbacks can reduce the antioxidant efficiency of α-LA and so the application of α-LA as a food supplement will be limited without protection. Nevertheless, there are studies in the literature in which α-LA was encapsulated into CyD cavities to enhance its water solubility and increase thermal/light stability by inclusion complexation.[10−16] Here, water solubility and thermal stability enhancement of α-LA in α-LA/CyD NF web were demonstrated by TGA analysis and solubility tests. Additionally, antioxidant property of α-LA powder and α-LA/CyD NF web was evaluated using (2,2′-azinobis (3-ethyl-benzothiazoline-6-sulfonate)) radical cation ($ABTS^{\bullet+}$) scavenging assay. Since $ABTS^{\bullet+}$ technique is applicable in both lipid and aqueous phases, it is widely used to examine the antioxidant property of many products including beverages, essential oils, fruits, vegetables, etc.[57,58] In this technique, an $ABTS^{\bullet+}$ solution having blue-green color is obtained by the oxidation of ABTS using potassium persulfate. Afterward, the antioxidant activity of the product is monitored spectrophotometrically by following the decolorization of the $ABTS^{\bullet+}$ solution upon the

DOI: 10.1021/acs.jafc.9b05580
J. Agric. Food Chem. XXXX, XXX, XXX−XXX

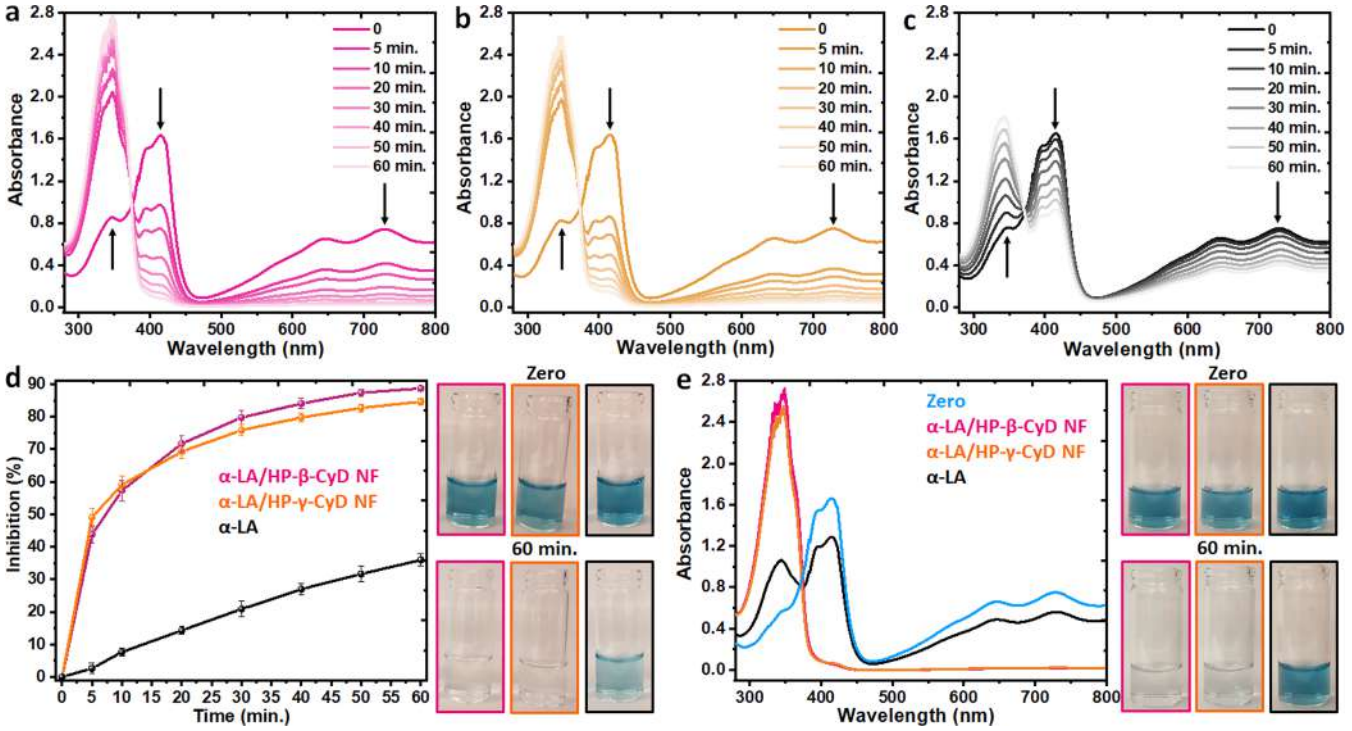

Figure 9. UV−vis spectra showing time dependent ABTS$^{\bullet+}$ scavenging performance of (a) α-LA/HP-β-CyD NF web, (b) α-LA/HP-γ-CyD NF web, and (c) pure α-LA. (d) Time dependent inhibition (%) graphs and photographs of solutions of α-LA/HP-β-CyD NF, α-LA/HP-γ-CyD NF web, and pure α-LA. (e) UV−vis spectra and photographs of solutions of α-LA/HP-β-CyD NF, α-LA/HP-γ-CyD NF web, and pure α-LA indicating the antioxidant performance after heat treatment (100 °C for 24 h).

reduction of radical cation to ABTS.[57−59] Figure 9 shows the time dependent radical scavenging test results of pure α-LA, α-LA/HP-β-CyD NF, and α-LA/HP-γ-CyD NF webs. Here, the same amount of α-LA/HP-β-CyD NF (∼20 mg) and α-LA/HP-γ-CyD NF (∼20 mg) sample were used to perform the antioxidant activity tests. As a control sample, pure α-LA was weighted according to α-LA content of α-LA/HP-β-CyD NF web (∼2.5 mg) because it has slightly higher loading of α-LA compared to α-LA/HP-γ-CyD NF web (∼2.0 mg) which was proved by ^{1}H NMR analysis. Since ABTS$^{\bullet+}$ assay is applicable in aqueous medium, ABTS$^{\bullet+}$ solution is directly mixed with samples and the inhibition profile was recorded for progressing time intervals (Figure 9a-d). Due to rapid dissolution property, α-LA/CyD NF webs immediately dissolved upon the contact with ABTS$^{\bullet+}$ solution, in contrast α-LA powder remains in the solutions without dissolving. The UV−vis measurements of pure α-LA, α-LA/HP-β-CyD NF and α-LA/HP-γ-CyD NF systems were completed in 60 min. (Figure 9a-c) and Figure 9d displays the time dependent ABTS$^{\bullet+}$ scavenging graphs and photographs of the solutions for all samples. Here, the absorbance of the stock solution was concurrently measured with the samples and the inhibition percentage of each samples was calculated considering the decrease at the reference absorbance intensity (734 nm) which is originated from the stock solution decolorization. The UV−vis spectra, time dependent inhibition (%) graphs and the solution photographs clearly indicate the differences between antioxidant performance of pure α-LA and α-LA/CyD NF webs. Despite the same amount of α-LA was used as in α-LA/HP-β-CyD NF web and higher amount of α-LA was used than α-LA/HP-γ-CyD NF web, pure α-LA represented significantly lower radical scavenging efficiency compared α-LA/CyD NF webs in the given time period. While α-LA/HP-β-CyD NF and α-LA/HP-γ-CyD NF indicate ∼89% and ∼85% inhibition activity, respectively, pure α-LA indicates ∼36% inhibition activity in 60 min, under the same conditions. Even, α-LA/CyD NF completed ∼50% of radical scavenging in the first 5 min of the reaction period. Therefore, it is also concluded that α-LA/CyD NF webs provide faster scavenging performance compared to pure α-LA (Figure 9d). The superior antioxidant property of α-LA in α-LA/CyD NF webs is due to enhanced water solubility of α-LA by inclusion complexation in which more amount of α-LA become water-soluble and could participate in the scavenging of ABTS$^{\bullet+}$. As seen in Figure 9d, there is no significant difference between the inhibition rates of α-LA/HP-β-CyD NF and α-LA/HP-γ-CyD NF, but α-LA/HP-β-CyD NF show slightly higher inhibition activity compared to α-LA/HP-γ-CyD NF possibly due to the higher α-LA content. Our recent findings agree with the results has been noted by others and in our previous studies in which the antioxidant property of different active compound was improved by the inclusion complexation with different types of CyD molecules.[30−32] In one of the related studies, Lucas-Abellán et al. showed the enhanced antioxidant activity of resveratrol in the presence of CyD.[60] In addition, Kfoury et al. found that the inclusion complexation improves the antiradical activity of essential oils.[8] It should be noted that, the absorbance of ABTS$^{\bullet+}$ also decreases (30−47%) when the experiment was performed with pristine HP-β-CyD NF and HP-γ-CyD NF alone and this result is in correlation with the literature.[60,61] In these related reports, the decay of the ABTS$^{\bullet+}$ absorbance was monitored with the increasing concentration of HP-β-CyD and this was attributed to formation of inclusion complex between the cationic radical of ABTS and CyD molecules.[60,61] The enhanced thermal stability of α-LA was also demonstrated with antioxidant activity assay. For this, same amounts of

DOI: 10.1021/acs.jafc.9b05580
J. Agric. Food Chem. XXXX, XXX, XXX−XXX

samples with the antioxidant test (α-LA (~2.5 mg), α-LA/HP-β-CyD NF (~20 mg), and α-LA/HP-γ-CyD NF (~20 mg)) were prepared and then exposed to further heat treatment at 100 °C for 24 h. Afterward, samples were mixed with diluted $ABTS^{\bullet+}$ solution and incubated at room temperature for 60 min prior to UV−vis measurement. Figure 9e shows the UV−vis absorbance and the photographs of the sample solutions of α-LA, α-LA/HP-β-CyD NF, and α-LA/HP-γ-CyD NF. While α-LA/HP-β-CyD NF and α-LA/HP-γ-CyD NF demonstrated the similar antioxidant performance after the heat treatment (~90% inhibition), there is a significant reduction at the antioxidant activity of pure α-LA (~17% inhibition). These results are correlated with the solubility test in which the absorbance intensity of pure α-LA decrease approximately 42% compared to its initial state, since the poor thermal stability of α-LA probably lead to degradation/polymerization of α-LA by the thermal treatment. Nevertheless, for α-LA/CyD NF web samples, encapsulation of α-LA in CyD cavity protects it against heat and maintains its antioxidant property despite exposing high temperature (100 °C) for 24 h. Both the solubility and antioxidant test endorsed the stabilizing and performance enhancing effect of CyD inclusion complexation on α-LA properties.

To conclude, cyclodextrins (CyDs) are quite effective for enhancing the water solubility, thermal stability, and bioavailability of essential oils, vitamins, flavors, food supplements, etc., by forming inclusion complexes. On the other hand, electrospinning is a very promising technique for the encapsulation of all these bioactive compounds. Therefore, encapsulation of bioactive compounds by electrospinning of their CyD inclusion complexes is an attractive approach for food applications. Here, the highly water-soluble CyD derivates of HP-β-CyD and HP-γ-CyD were chosen as both fiber matrix and inclusion complexation agent in order to improve the water-solubility, high temperature stability and antioxidant activity of alpha-lipoic acid (α-LA). The electrospinning of α-LA/CyD aqueous systems was successfully performed without any additional fiber forming polymeric matrix and, α-LA/HP-β-CyD and α-LA/HP-γ-CyD nanofibers in the form of nanofibrous webs were produced. The initial molar ratio (1/1) of α-LA/CyD systems was mostly protected during the electrospinning process, therefore inclusion complex nanofibers of α-LA/CyD were successfully produced with high loading (~10−12% (w/w)) of α-LA. Moreover, α-LA/CyD complexes became more favorable for the practical applications compared to its powder form due to self-standing, flexible and foldable properties of α-LA/CyD nanofibrous webs. The α-LA/CyD nanofibrous webs have very fast dissolving property in water and when wetted in artificial saliva, which suggest promising potential for α-LA/CyD nanofibrous webs as orally fast-dissolving systems for food supplements. It is also important to state that the electrospinning of α-LA/CyD nanofibers was performed in water since α-LA become water-soluble by CyD and the use of water is very advantageous for the industrial processing of active agents/CyD inclusion complex nanofibers. The inclusion complex nanofibers of α-LA/CyD also provided an enhanced thermal stability and antioxidant property, which paves the way for practical use of α-LA as food supplement. Further, CyDs are used for inclusion complexation with variety of bioactive agents, so many other food supplements or bioactive compounds can be used for the development of orally fast-dissolving films/membranes/mats from CyD inclusion complex nanofibers by electrospinning.

■ ASSOCIATED CONTENT

Supporting Information

The Supporting Information is available free of charge on the ACS Publications website at DOI: 10.1021/acs.jafc.9b05580.

Photographs of α-LA/CyD nanofibrous webs after 2 months stored at 55−65% RH and 22 °C (Figure S1a) and UV−vis spectra of aqueous solutions of α-LA/CyD nanofibers after 2 months of storage (Figure S1b) (PDF)

Comparative dissolution profile of α-LA powder, CyD NF and α-LA/CyD NF webs. (AVI)

Disintegration profile of α-LA/CyD NF webs. (AVI)

■ AUTHOR INFORMATION

Corresponding Authors

*E-mail: ac2873@cornell.edu.

*E-mail: tu46@cornell.edu.

ORCID

Asli Celebioglu: 0000-0002-5563-5746

Tamer Uyar: 0000-0002-3989-4481

Author Contributions

T. U. and A.C. designed the study, wrote the manuscript, and have given approval to the final version of the manuscript. A.C. performed the experimental studies.

Notes

The authors declare no competing financial interest.

■ ACKNOWLEDGMENTS

This work made use of the Cornell Center for Materials Research Shared Facilities which are supported through the NSF MRSEC program (DMR-1719875), and the Cornell Chemistry NMR Facility supported in part by the NSF MRI program (CHE-1531632), and the Department of Fiber Science & Apparel Design facilities. Prof. Uyar acknowledges the startup funding from the College of Human Ecology at Cornell University. The partial funding for this research was also graciously provided by Nixon Family (Lea and John Nixon) thru College of Human Ecology at Cornell University.

■ REFERENCES

(1) Packer, L.; Witt, E. H.; Tritschler, H. J. Alpha-Lipoic Acid as a Biological Antioxidant. *Free Radical Biol. Med.* **1995**, *19*, 227−250.

(2) Gorąca, A.; Huk-Kolega, H.; Piechota, A.; Kleniewska, P.; Ciejka, E.; Skibska, B. Lipoic Acid−Biological Activity and Therapeutic Potential. *Pharmacol. Rep.* **2011**, *63*, 849−858.

(3) Shay, K. P.; Moreau, R. F.; Smith, E. J.; Smith, A. R.; Hagen, T. M. Alpha-Lipoic Acid as a Dietary Supplement: Molecular Mechanisms and Therapeutic Potential. *Biochim. Biophys. Acta, Gen. Subj.* **2009**, *1790*, 1149−1160.

(4) Li, Y.-X.; Park, E. Y.; Lim, S.-T. Stabilization of Alpha-Lipoic Acid by Complex Formation with Octenylsuccinylated High Amylose Starch. *Food Chem.* **2018**, *242*, 389−394.

(5) Li, Y.-X.; Kim, Y.-J.; Reddy, C. K.; Lee, S.-J.; Lim, S.-T. Enhanced Bioavailability of Alpha-Lipoic Acid by Complex Formation with Octenylsuccinylated High-Amylose Starch. *Carbohydr. Polym.* **2019**, *219*, 39−45.

(6) Marques, H. M. C. A Review on Cyclodextrin Encapsulation of Essential Oils and Volatiles. *Flavour Fragrance J.* **2010**, *25*, 313−326.

DOI: 10.1021/acs.jafc.9b05580
J. Agric. Food Chem. XXXX, XXX, XXX−XXX

(7) Fenyvesi, E.; Vikmon, M.; Szente, L. Cyclodextrins in Food Technology and Human Nutrition: Benefits and Limitations. *Crit. Rev. Food Sci. Nutr.* **2016**, *56*, 1981−2004.
(8) Kfoury, M.; Auezova, L.; Greige-Gerges, H.; Fourmentin, S. Promising Applications of Cyclodextrins in Food: Improvement of Essential Oils Retention, Controlled Release and Antiradical Activity. *Carbohydr. Polym.* **2015**, *131*, 264−272.
(9) Astray, G.; Gonzalez-Barreiro, C.; Mejuto, J. C.; Rial-Otero, R.; Simal-Gandara, J. A Review on the Use of Cyclodextrins in Foods. *Food Hydrocolloids* **2009**, *23*, 1631−1640.
(10) Ikuta, N.; Terao, K.; Matsugo, S. Stabilized R-α-Lipoic Acid by Encapsulation Using Cyclodextrins. In *Impact of Nanoscience in the Food Industry*; Elsevier: Amsterdam, 2018; pp 351−366.
(11) Noothalapati, H.; Ikarashi, R.; Iwasaki, K.; Nishida, T.; Kaino, T.; Yoshikiyo, K.; Terao, K.; Nakata, D.; Ikuta, N.; Ando, M. Studying Anti-Oxidative Properties of Inclusion Complexes of α-Lipoic Acid with γ-Cyclodextrin in Single Living Fission Yeast by Confocal Raman Microspectroscopy. *Spectrochim. Acta, Part A* **2018**, *197*, 237−243.
(12) Caira, M.; Bourne, S.; Mzondo, B. Encapsulation of the Antioxidant R-(+)-α-Lipoic Acid in Permethylated α-and β-Cyclodextrins: Thermal and X-Ray Structural Characterization of the 1:1 Inclusion Complexes. *Molecules* **2017**, *22*, 866.
(13) Ikuta, N.; Okamoto, H.; Furune, T.; Uekaji, Y.; Terao, K.; Uchida, R.; Iwamoto, K.; Miyajima, A.; Hirota, T.; Sakamoto, N. Bioavailability of an R-α-Lipoic Acid/γ-Cyclodextrin Complex in Healthy Volunteers. *Int. J. Mol. Sci.* **2016**, *17*, 949.
(14) Uchida, R.; Iwamoto, K.; Nagayama, S.; Miyajima, A.; Okamoto, H.; Ikuta, N.; Fukumi, H.; Terao, K.; Hirota, T. Effect of γ-Cyclodextrin Inclusion Complex on the Absorption of R-α-Lipoic Acid in Rats. *Int. J. Mol. Sci.* **2015**, *16*, 10105−10120.
(15) Ikuta, N.; Sugiyama, H.; Shimosegawa, H.; Nakane, R.; Ishida, Y.; Uekaji, Y.; Nakata, D.; Pallauf, K.; Rimbach, G.; Terao, K. Analysis of the Enhanced Stability of R (+)-Alpha Lipoic Acid by the Complex Formation with Cyclodextrins. *Int. J. Mol. Sci.* **2013**, *14*, 3639−3655.
(16) Takahashi, H.; Bungo, Y.; Mikuni, K. The Aqueous Solubility and Thermal Stability of α-Lipoic Acid Are Enhanced by Cyclodextrin. *Biosci., Biotechnol., Biochem.* **2011**, *75*, 1102282391.
(17) Maeda, H.; Onodera, T.; Nakayama, H. Inclusion Complex of α-Lipoic Acid and Modified Cyclodextrins. *J. Inclusion Phenom. Mol. Recognit. Chem.* **2010**, *68*, 201−206.
(18) Bhushani, J. A.; Anandharamakrishnan, C. Electrospinning and Electrospraying Techniques: Potential Food Based Applications. *Trends Food Sci. Technol.* **2014**, *38*, 21−33.
(19) Wen, P.; Wen, Y.; Zong, M.-H.; Linhardt, R. J.; Wu, H. Encapsulation of Bioactive Compound in Electrospun Fibers and Its Potential Application. *J. Agric. Food Chem.* **2017**, *65*, 9161−9179.
(20) Rostami, M. R.; Yousefi, M.; Khezerlou, A.; Mohammadi, M. A.; Jafari, S. M. Application of Different Biopolymers for Nano-encapsulation of Antioxidants via Electrohydrodynamic Processes. *Food Hydrocolloids* **2019**, *97*, 105170.
(21) Wen, P.; Zong, M.-H.; Linhardt, R. J.; Feng, K.; Wu, H. Electrospinning: A Novel Nano-Encapsulation Approach for Bioactive Compounds. *Trends Food Sci. Technol.* **2017**, *70*, 56−68.
(22) Leidy, R.; Ximena, Q.-C. M. Use of Electrospinning Technique to Produce Nanofibres for Food Industries: A Perspective from Regulations to Characterisations. *Trends Food Sci. Technol.* **2019**, *85*, 92−106.
(23) Kumar, T. S. M.; Kumar, K. S.; Rajini, N.; Siengchin, S.; Ayrilmis, N.; Rajulu, A. V. A Comprehensive Review of Electrospun Nanofibers: Food and Packaging Perspective. *Composites, Part B* **2019**, *175*, 107074.
(24) Jafari, S. M. An Overview of Nanoencapsulation Techniques and Their Classification. In *Nanoencapsulation technologies for the food and nutraceutical industries*; Elsevier: Amsterdam, 2017; pp 1−34.
(25) Yu, D.-G.; Li, J.-J.; Williams, G. R.; Zhao, M. Electrospun Amorphous Solid Dispersions of Poorly Water-Soluble Drugs: A Review. *J. Controlled Release* **2018**, *292*, 91−110.
(26) Aytac, Z.; Ipek, S.; Erol, I.; Durgun, E.; Uyar, T. Fast-Dissolving Electrospun Gelatin Nanofibers Encapsulating Ciprofloxacin/Cyclodextrin Inclusion Complex. *Colloids Surf., B* **2019**, *178*, 129−136.
(27) Aytac, Z.; Celebioglu, A.; Yildiz, Z.; Uyar, T. Efficient Encapsulation of Citral in Fast-Dissolving Polymer-Free Electrospun Nanofibers of Cyclodextrin Inclusion Complexes: High Thermal Stability, Longer Shelf-Life, and Enhanced Water Solubility of Citral. *Nanomaterials* **2018**, *8*, 793.
(28) Yildiz, Z. I.; Celebioglu, A.; Kilic, M. E.; Durgun, E.; Uyar, T. Fast-Dissolving Carvacrol/Cyclodextrin Inclusion Complex Electrospun Fibers with Enhanced Thermal Stability, Water Solubility, and Antioxidant Activity. *J. Mater. Sci.* **2018**, *53*, 15837−15849.
(29) Yildiz, Z. I.; Celebioglu, A.; Kilic, M. E.; Durgun, E.; Uyar, T. Menthol/Cyclodextrin Inclusion Complex Nanofibers: Enhanced Water-Solubility and High-Temperature Stability of Menthol. *J. Food Eng.* **2018**, *224*, 27−36.
(30) Celebioglu, A.; Uyar, T. Antioxidant Vitamin E/Cyclodextrin Inclusion Complex Electrospun Nanofibers: Enhanced Water Solubility, Prolonged Shelf Life, and Photostability of Vitamin E. *J. Agric. Food Chem.* **2017**, *65*, 5404−5412.
(31) Celebioglu, A.; Yildiz, Z. I.; Uyar, T. Thymol/Cyclodextrin Inclusion Complex Nanofibrous Webs: Enhanced Water Solubility, High Thermal Stability and Antioxidant Property of Thymol. *Food Res. Int.* **2018**, *106*, 280−290.
(32) Celebioglu, A.; Yildiz, Z. I.; Uyar, T. Fabrication of Electrospun Eugenol/Cyclodextrin Inclusion Complex Nanofibrous Webs for Enhanced Antioxidant Property, Water Solubility, and High Temperature Stability. *J. Agric. Food Chem.* **2018**, *66*, 457−466.
(33) Celebioglu, A.; Aytac, Z.; Kilic, M. E.; Durgun, E.; Uyar, T. Encapsulation of Camphor in Cyclodextrin Inclusion Complex Nanofibers via Polymer-Free Electrospinning: Enhanced Water Solubility, High Temperature Stability, and Slow Release of Camphor. *J. Mater. Sci.* **2018**, *53*, 5436−5449.
(34) Celebioglu, A.; Yildiz, Z. I.; Uyar, T. Electrospun Nanofibers from Cyclodextrin Inclusion Complexes with Cineole and P-cymene: Enhanced Water Solubility and Thermal Stability. *Int. J. Food Sci. Technol.* **2018**, *53*, 112−120.
(35) Aytac, Z.; Yildiz, Z. I.; Kayaci-Senirmak, F.; Tekinay, T.; Uyar, T. Electrospinning of Cyclodextrin/Linalool-Inclusion Complex Nanofibers: Fast-Dissolving Nanofibrous Web with Prolonged Release and Antibacterial Activity. *Food Chem.* **2017**, *231*, 192−201.
(36) Aytac, Z.; Yildiz, Z. I.; Kayaci-Senirmak, F.; San Keskin, N. O.; Kusku, S. I.; Durgun, E.; Tekinay, T.; Uyar, T. Fast-Dissolving, Prolonged Release, and Antibacterial Cyclodextrin/Limonene-Inclusion Complex Nanofibrous Webs via Polymer-Free Electrospinning. *J. Agric. Food Chem.* **2016**, *64*, 7325−7334.
(37) Aytac, Z.; Yildiz, Z. I.; Kayaci-Senirmak, F.; San Keskin, N. O.; Tekinay, T.; Uyar, T. Electrospinning of Polymer-Free Cyclodextrin/Geraniol−Inclusion Complex Nanofibers: Enhanced Shelf-Life of Geraniol with Antibacterial and Antioxidant Properties. *RSC Adv.* **2016**, *6*, 46089−46099.
(38) Celebioglu, A.; Kayaci-Senirmak, F.; Ipek, S.; Durgun, E.; Uyar, T. Polymer-Free Nanofibers from Vanillin/Cyclodextrin Inclusion Complexes: High Thermal Stability, Enhanced Solubility and Antioxidant Property. *Food Funct.* **2016**, *7*, 3141−3153.
(39) Szente, L.; Szejtli, J. Highly Soluble Cyclodextrin Derivatives: Chemistry, Properties, and Trends in Development. *Adv. Drug Delivery Rev.* **1999**, *36*, 17−28.
(40) Celebioglu, A.; Uyar, T. Electrospinning of Nanofibers from Non-Polymeric Systems: Polymer-Free Nanofibers from Cyclodextrin Derivatives. *Nanoscale* **2012**, *4*, 621−631.
(41) Rostami, M.; Ghorbani, M.; Delavar, M.; Tabibiazar, M.; Ramezani, S. Development of Resveratrol Loaded Chitosan-Gellan Nanofiber as a Novel Gastrointestinal Delivery System. *Int. J. Biol. Macromol.* **2019**, *135*, 698−705.
(42) Higuchi, T.; Connors, K. A. Phase Solubility Diagram. *Adv. Anal Chem. Instrum* **1965**, *4*, 117−212.
(43) Bi, Y.; Sunada, H.; Yonezawa, Y.; Danjo, K.; Otsuka, A.; Iida, K. Preparation and Evaluation of a Compressed Tablet Rapidly

DOI: 10.1021/acs.jafc.9b05580
J. Agric. Food Chem. XXXX, XXX, XXX−XXX

Disintegrating in the Oral Cavity. *Chem. Pharm. Bull.* **1996**, *44*, 2121−2127.
(44) Topuz, F.; Uyar, T. Influence of Hydrogen-Bonding Additives on Electrospinning of Cyclodextrin Nanofibers. *ACS Omega* **2018**, *3*, 18311−18322.
(45) Uyar, T.; Besenbacher, F. Electrospinning of Uniform Polystyrene Fibers: The Effect of Solvent Conductivity. *Polymer* **2008**, *49*, 5336−5343.
(46) Racz, C.-P.; Santa, S.; Tomoaia-Cotisel, M.; Borodi, G.; Kacso, I.; Pirnau, A.; Bratu, I. Inclusion of α-Lipoic Acid in β-Cyclodextrin. Physical−Chemical and Structural Characterization. *J. Inclusion Phenom. Mol. Recognit. Chem.* **2013**, *76*, 193−199.
(47) Mura, P. Analytical Techniques for Characterization of Cyclodextrin Complexes in the Solid State: A Review. *J. Pharm. Biomed. Anal.* **2015**, *113*, 226−238.
(48) Narayanan, G.; Boy, R.; Gupta, B. S.; Tonelli, A. E. Analytical Techniques for Characterizing Cyclodextrins and Their Inclusion Complexes with Large and Small Molecular Weight Guest Molecules. *Polym. Test.* **2017**, *62*, 402−439.
(49) Hădărugă, N. G.; Bandur, G. N.; David, I.; Hădărugă, D. I. A Review on Thermal Analyses of Cyclodextrins and Cyclodextrin Complexes. *Environ. Chem. Lett.* **2019**, *17*, 349−373.
(50) Schönbeck, C.; Madsen, T. L.; Peters, G. H.; Holm, R.; Loftsson, T. Soluble 1:1 Complexes and Insoluble 3:2 Complexes − Understanding the Phase-Solubility Diagram of Hydrocortisone and γ-Cyclodextrin. *Int. J. Pharm.* **2017**, *531*, 504−511.
(51) Brewster, M. E.; Loftsson, T. Cyclodextrins as Pharmaceutical Solubilizers. *Adv. Drug Delivery Rev.* **2007**, *59*, 645−666.
(52) Loftsson, T.; Frikdriksdóttir, H.; Sigurkdardóttir, A. M.; Ueda, H. The Effect of Water-Soluble Polymers on Drug-Cyclodextrin Complexation. *Int. J. Pharm.* **1994**, *110*, 169−177.
(53) Loftsson, T.; Brewster, M. E. Pharmaceutical Applications of Cyclodextrins: Basic Science and Product Development. *J. Pharm. Pharmacol.* **2010**, *62*, 1607−1621.
(54) Seifar, F.; Khalili, M.; Khaledyan, H.; Amiri Moghadam, S.; Izadi, A.; Azimi, A.; Shakouri, S. K. α-Lipoic Acid, Functional Fatty Acid, as a Novel Therapeutic Alternative for Central Nervous System Diseases: A Review. *Nutr. Neurosci.* **2019**, *22*, 306−316.
(55) Firuzi, O.; Miri, R.; Tavakkoli, M.; Saso, L. Antioxidant Therapy: Current Status and Future Prospects. *Curr. Med. Chem.* **2011**, *18*, 3871−3888.
(56) Rochette, L.; Ghibu, S.; Richard, C.; Zeller, M.; Cottin, Y.; Vergely, C. Direct and Indirect Antioxidant Properties of α-Lipoic Acid and Therapeutic Potential. *Mol. Nutr. Food Res.* **2013**, *57*, 114−125.
(57) Moon, J. K.; Shibamoto, T. Antioxidant Assays for Plant and Food Components. *J. Agric. Food Chem.* **2009**, *57*, 1655−1666.
(58) Gülçin, I. Antioxidant Activity of Food Constituents: An Overview. *Arch. Toxicol.* **2012**, *86*, 345−391.
(59) Sánchez, C. Reactive Oxygen Species and Antioxidant Properties from Mushrooms. *Synth. Syst. Biotechnol.* **2017**, *2*, 13−22.
(60) Lucas-Abellán, C.; Mercader-Ros, M. T.; Zafrilla, M. P.; Gabaldón, J. A.; Núñez-Delicado, E. Comparative Study of Different Methods to Measure Antioxidant Activity of Resveratrol in the Presence of Cyclodextrins. *Food Chem. Toxicol.* **2011**, *49*, 1522−1260.
(61) Kfoury, M.; Landy, D.; Ruellan, S.; Auezova, L.; Greige-Gerges, H.; Fourmentin, S. Determination of Formation Constants and Structural Characterization of Cyclodextrin Inclusion Complexes with Two Phenolic Isomers: Carvacrol and Thymol. *Beilstein J. Org. Chem.* **2016**, *12*, 29−42.

DOI: 10.1021/acs.jafc.9b05580
J. Agric. Food Chem. XXXX, XXX, XXX−XXX